Least-squares pressure recovery in reduced order methods for incompressible flows

Mejdi Azaiez, T. Chacón Rebollo, M. Oulghelou, I. Sánchez Muñoz

Least-squares pressure recovery in Reduced Order Methods for incompressible flows

M. Azaïez[*] T. Chacón Rebollo [†] M. Oulghelou [‡] I. Sánchez Muñoz [§]

November 13, 2024

Abstract

In this work, we introduce a method to recover the reduced pressure for Reduced Order Models (ROMs) of incompressible flows. The pressure is obtained as the least-squares minimum of the residual of the reduced velocity with respect to a dual norm. We prove that this procedure provides a unique solution whenever the full-order pair of velocity-pressure spaces is inf-sup stable. We also prove that the proposed method is equivalent to solving the reduced mixed problem with reduced velocity basis enriched with the supremizers of the reduced pressure gradients. Optimal error estimates for the reduced pressure are obtained for general incompressible flow equations and specifically, for the transient Navier-Stokes equations. We also perform some numerical tests for the flow past a cylinder and the lid-driven cavity flow which confirm the theoretical expectations, and show an improved convergence with respect to other pressure recovery methods.

Keywords: Pressure recovery, Inf-sup condition, Reduced Order Methods, Incompressible flow, Navier-Stokes equations

1 Introduction

Apart from addressing the non-linear convective term, the primary challenge in numerically solving the time-dependent, incompressible Navier-Stokes equations lies in the Stokes stage. Specifically, determining the pressure field acts as a Lagrange multiplier to ensure the continuity equation. This issue has led to a significant body of work and publications in both non-reduced and reduced-order methods. In the non-reduced framework, two main families of approaches can be considered: one based on time splitting and the projection method. For comprehensive coverage on this topic, refer to the following references [11, 23]. The second family of methods operates without splitting and utilizes techniques such as Uzawa algorithms. For further insights, consult the following references [9, 24, 29]. The challenge of pressure calculation persists in the numerical solution of the Navier-Stokes equations using reduced bases. According to our review of the literature, solutions to this issue depend on the nature of the vectors in the bases of the reduced spaces, specifically on whether these vectors are divergence-free or not. For comments and justifications on this issue, refer, for example, to [3, 8, 16, 20] and the references therein. Indeed, if the reduced base only weakly satisfies the constraint, it becomes impossible to directly calculate the pressure, which is precisely the Lagrange

[*]Bordeaux University, Bordeaux INP and I2M (UMR CNRS 5295), 33400 Talence (France). azaiez@u-bordeaux.fr
[†]Departamento EDAN & IMUS, Universidad de Sevilla, Spain. chacon@us.es
[‡]Institut Jean Le rond d'Alembert, Sorbonne Universite, 4 Place Jussieu, Paris (France). mourad.oulghelou@upmc.fr
[§]Departamento Matemática Aplicada I, Universidad de Sevilla, Spain. isanchez@us.es

multiplier in the equations ensuring the constraint, using the Galerkin-POD-ROM application.
To overcome this challenge, various methods have been proposed to recover the pressure of the reduced model a posteriori. These include:

i) solving the Poisson pressure equation (PPE) with appropriate boundary conditions. In this formula, the continuity equation of the reduced system is replaced by the Poisson pressure equation, which is obtained by taking the divergence of the momentum equation and exploiting the fact that the velocity field is divergence-free. For the Poisson equation to be consistent with the initial NSE, we need to impose appropriate boundary conditions. Some possibilities include enforcing a no-slip boundary on the velocity, or incorporating a Neumann boundary condition, which in some cases leads to an artificial boundary layer. Full details of these different approaches can be found in [2, 13, 19, 20, 28]. More recently, in [6], the authors proposed to solve a pressure equation by duality with the gradients of the reduced pressure basis functions. This amounts to solving a Poisson equation for the pressure, with the advantage of defining better adapted boundary conditions and ensuring better precision in their recovery. However, their approach does not seem to provide a clear answer for the case of non-ordinary boundary conditions, such as the non-stress or outflow boundary condition. Finally, it is important to note another inconsistency in the choice of the H^1 regularity of the pressure to solve the Poisson problem compared to that of NS, where the pressure is only L^2.

ii) solving the pressure via the momentum equation recovery formulation

$$\nabla p_r = \mathbf{f} - \partial_{\mathbf{t}} \boldsymbol{u}_{\mathbf{r}} \ldots.$$

In practice, additional velocity space modes, called supremizer modes, are introduced to compute the reduced pressure. They are chosen to satisfy the inf-sup condition [3, 4, 12, 26]. This approach to pressure recovery was introduced in the context of the POD for parameterised NSEs (see [3]) . A stability analysis in terms of the existence of an inf-sup condition was carried out in the same reference. The method was later extended in [30] to the case where a strongly divergence-free POD velocity basis is used. It has also been used in the context of Petrov-Galkerin methods in [1, 7].The way to ensure a stable enrichment of the reduced velocity basis is to go through each element of the reduced pressure basis and compute the Riesz representation of the linear, continuous functional associated with the gradient of it. It is obtained by solving a vectoriel Poisson problem with as right hand side the gradient of the pressure element. More recently, in [15], data-driven closure/correction terms are given and studied to increase the pressure and velocity accuracy of reduced order models (ROMs) for fluid flows. These references propose some supremiser stabilisation techniques to ensure compatibility between the pressure and added velocity spaces. In [16], the authors proposed a numerical analysis of the two approaches. They proved stability and convergence results for the supremizer-stabilised approach and numerically investigated these properties, in addition to its performance against the pressure Poisson method.

In this paper, we propose an approach falling into category (ii). We adopt a strategy that has the dual advantage of calculating pressure without resorting to additional boundary conditions and extending the choice of velocities in the supermizers procedure. We propose a recovery procedure using least-squares minimization of the residual dual norm. We prove that this procedure provides a unique solution whenever the full-order pair of velocity-pressure spaces is inf-sup stable. Additionally, we establish that this least-squares recovery of the pressure is equivalent to solving the reduced mixed

problem with the reduced velocity basis enriched with the supremizers of the reduced pressure gradients. In essence, the pressure computed by the supremizers procedure is treated as the least-squares pressure provided by the velocity solution of the reduced mixed problem. A similar result holds for the full-order mixed problem. As a consecuence, the reduced pressure obtained by the least-squares method is equivalent to the pressure obtained from MER formulation with suprermizers as test functions, which has been studied in [8, 16]. We also prove error estimates for the least-squares recovered pressure for general incompressible flow equations. Finally, we present numerical results for transient Navier-Stokes equations, demonstrating good agreement with theoretical expectations. We obtain discretization errors in the approximation of the reduced pressure quite close to the POD projection, achieving error reductions of four orders of magnitude compared to the pressure Poisson Equation approach.

The following sections of this paper are organized as follows: in Section 2, we introduce the parametrized incompressible Navier-Stokes equation and derive its reduced-order Galerkin formulation. Moving on to Section 3, we describe the reduced pressure recovery through the least-squares minimum residual, analyzing the existence and uniqueness of the solution. This section concludes with an algebraic description of the operator on the pressure. Section 4 establishes the equivalence between the pressure gradient supremizers procedure and the least-squares recovery of the pressure, along with exploring the adoption of a new choice of supremizers procedure. Optimal error estimates for the pressure, in terms of the approximation, are proven in Section 5. In Section 6, we conduct a numerical investigation into the performance of these pressure recovery techniques. Numerical tests are performed to assess and quantify the error estimates derived in the previous section for the pressure, and a comparison is made with the results obtained by the method introduced by Chacon et al (refer to [6]).

2 The need of pressure recovery for ROMs of incompressible flows

We start from a ROM for an incompressible flow that is solved only for velocity, dropping the free divergence equation. To describe it, we consider a boundary value parametric model for the incompressible Navier-Stokes-Brinkman. Set $\Omega \subset \mathbb{R}^d$ ($d = 2$ or 3) be a bounded domain with a Lipschitz-continuous boundary $\Gamma = \partial\Omega$ which is splitted into two disjoint parts $\Gamma = \Gamma_D \cup \Gamma_N$. We consider the problem:

Find a velocity field $\boldsymbol{u}(\mu) : \Omega \to \mathbb{R}^d$ *and a pressure* $p(\mu) : \Omega \to \mathbb{R}$ *such that*

$$\begin{cases} \gamma\, \boldsymbol{u}(\mu) + \boldsymbol{u}(\mu) \cdot \nabla \boldsymbol{u}(\mu) - \mu \Delta \boldsymbol{u}(\mu) + \nabla p(\mu) = \boldsymbol{f} & \text{in } \Omega, \\ \nabla \cdot \boldsymbol{u}(\mu) = 0 & \text{in } \Omega, \\ \boldsymbol{u}(\mu) = \boldsymbol{0} & \text{on } \Gamma_D, \\ -\mu\, \partial_{\boldsymbol{n}} \boldsymbol{u}(\mu) + p(\mu)\boldsymbol{n} = \boldsymbol{0} & \text{on } \Gamma_N, \end{cases} \tag{1}$$

where γ is a positive constant, $\boldsymbol{f} : \Omega \to \mathbb{R}^d$ is a given external body force field per unit mass and $\boldsymbol{n}$ is the external normal unit vector on Γ. Here $\mu = \frac{1}{Re}$, where Re is the Reynolds number, is considered as a parameter. In order to present the basic ideas of the pressure recovery method that we are going to introduce in this paper, we will consider a steady-state problem that depends on a single parameter with homogeneous boundary conditions. It can easily be extended to the transient problem depending on different parameters, either physical or geometrical or both, and more general boundary conditions. In fact, the first term in the first equation of the model includes the case of the evolution problem, once it has been discretised in time.

In order to formulate problem (1) in weak form we introduce for the velocity the space

$$\mathbf{H}^1_D(\Omega) = \left\{ \boldsymbol{v} \in H^1(\Omega)^d \text{ such that } \boldsymbol{v} = \boldsymbol{0} \text{ on } \Gamma_D \right\},$$

$\mathbf{H}^{-1}(\Omega)$ its dual space, while for the pressure we consider the space M that can be $L^2(\Omega)$ or $L^2_0(\Omega) = \left\{ q \in L^2(\Omega) \text{ such that } \int_\Omega q\, d\boldsymbol{x} = 0 \right\}$ when $\Gamma_N = \emptyset$. We denote by $(\cdot,\cdot)_0$ the L^2 inner product, either for scalar or vector functions, $(\cdot,\cdot)_1$ the inner product in $\mathbf{H}^1_D(\Omega)$. We also denote by $\|\cdot\|_0$ and $\|\cdot\|_1$ the norms defined by these inner products, respectively, and $\langle\cdot,\cdot\rangle$ the duality pairing between $\mathbf{H}^{-1}(\Omega)$ and $\mathbf{H}^1_D(\Omega)$.

The weak formulation of problem (1) consists in:

$$\begin{cases} \textit{Find } \boldsymbol{u}(\mu) \in \mathbf{H}^1_D(\Omega) \textit{ and } p(\mu) \in L^2_0(\Omega) \textit{ such that} \\ a(\boldsymbol{u}(\mu), \boldsymbol{u}(\mu), \boldsymbol{v}; \mu) - (\nabla \cdot \boldsymbol{v}, p(\mu))_0 = \langle \boldsymbol{f}, \boldsymbol{v} \rangle, \quad \forall\, \boldsymbol{v} \in \mathbf{H}^1_D(\Omega), \\ (\nabla \cdot \boldsymbol{u}(\mu), q)_0 = 0 \quad \forall\, q \in L^2_0(\Omega), \end{cases} \tag{2}$$

where a is the trilinear form given by

$$a(\boldsymbol{w}, \boldsymbol{u}, \boldsymbol{v}; \mu) = \gamma\, (\boldsymbol{u}, \boldsymbol{v})_0 + (\boldsymbol{w} \cdot \nabla \boldsymbol{u}, \boldsymbol{v})_0 + \mu\, (\nabla \boldsymbol{u}, \nabla \boldsymbol{v})_0, \quad \forall \boldsymbol{w}, \boldsymbol{u}, \boldsymbol{v} \in \mathbf{H}^1_D(\Omega).$$

To state the Galerkin discretisation of problem (2), let us consider a family of inf-sup stable discrete velocity-pressure spaces $(\boldsymbol{X}_h, M_h) \subset \mathbf{H}^1_D(\Omega) \times L^2_0(\Omega)$. That is, there exists a constant $\beta > 0$ such that

$$\beta\, \|q_h\|_0 \leq \sup_{\boldsymbol{v}_h \in \boldsymbol{X}_h} \frac{(\nabla \cdot \boldsymbol{v}_h, q_h)_0}{\|\nabla \boldsymbol{v}_h\|_0}, \quad \forall\, q_h \in M_h, \quad \forall\, h > 0. \tag{3}$$

Note that for some discretisation techniques, in particular for spectral methods, the constant β may depend on the discretisation parameter h.

We consider for instance the Galerkin discretisation of problem (2) (the "Full Order Model", FOM), that consists in:

$$\left\{\begin{array}{l} \textit{Find } \boldsymbol{u}_h(\mu) \in \boldsymbol{X}_h \textit{ and } p_h(\mu) \in M_h \textit{ such that} \\ a(\boldsymbol{u}_h(\mu), \boldsymbol{u}_h(\mu), \boldsymbol{v}_h; \mu) - (\nabla \cdot \boldsymbol{v}_h, p_h(\mu))_0 = \langle \boldsymbol{f}_h, \boldsymbol{v}_h \rangle, \quad \forall\, \boldsymbol{v}_h \in \boldsymbol{X}_h, \\ (\nabla \cdot \boldsymbol{u}_h(\mu), q_h)_0 = 0 \quad \forall\, q_h \in M_h, \end{array}\right. \tag{4}$$

where $\boldsymbol{f}_h$ is a given data coming from $\boldsymbol{f}$. For example, for the transient case, approximating the time evolution by a first-order Euler scheme then $\boldsymbol{f}_h = \boldsymbol{f} + \frac{1}{\Delta t}\boldsymbol{u}_h^{n-1}$.

To state the ROM approximation of problem (2), let us assume that we already have determined the reduced basis spaces for the discrete velocity and pressure $(\boldsymbol{X}_r, M_r)$, such that:

$$\boldsymbol{X}_r \subset \boldsymbol{X}_{0h} = \{\boldsymbol{v}_h \in \boldsymbol{X}_h \text{ such that } (\nabla \cdot \boldsymbol{v}_h, q_h) = 0,\, \forall q_h \in M_h\}. \tag{5}$$

We then consider the Galerkin projection of the momentum equation, as ROM for the velocity:

$$\left\{\begin{array}{l} \textit{Find } \boldsymbol{u}_r(\mu) \in \boldsymbol{X}_r \textit{ such that} \\ a(\boldsymbol{u}_r(\mu), \boldsymbol{u}_r(\mu), \boldsymbol{v}_r; \mu) = \langle \boldsymbol{f}_r, \boldsymbol{v}_r \rangle, \quad \forall\, \boldsymbol{v}_r \in \boldsymbol{X}_r, \end{array}\right. \tag{6}$$

where $\boldsymbol{f}_r$ is a reduced data coming from $\boldsymbol{f}$.

Note that the reduced pressure $p_r(\mu) \in M_r$ verifies $(\nabla \cdot \boldsymbol{v}_h,\, p_r(\mu)) = 0, \forall\, \boldsymbol{v}_h \in \boldsymbol{X}_{0h}$, because $M_r \subset M_h$, and thus the reduced pressure is removed from problem (6). However, this problem can be solved by itself, and only the reduced velocity is computed (as is done in practice for many engineering problems).

Nevertheless, for many applications in aerodynamics, hemodynamics and hydrodynamics, knowing the pressure is of paramount interest, to compute for instance drag and lift coefficients, or the pressure exerted by an artery on its walls. We will therefore tackle the problem of recovering the pressure from the velocity solution $\boldsymbol{u}_r(\mu)$ of the reduced problem (6).

3 Reduced pressure recovery by least-squares minimum residual

In the following, we omit the dependency of the reduced solution on the parameters for brevity.

The keystone of our method is to recover the reduced pressure by means of least-squares method. In order to describe it, let us introduce the following discrete operators:

$G : M_h \mapsto \mathbf{H}^{-1}(\Omega)$ given by

$$\langle G\, q_h, \boldsymbol{v}_h \rangle = -(\nabla \cdot \boldsymbol{v}_h, q_h)_0, \quad \forall q_h \in M_h,\, \forall \boldsymbol{v}_h \in \boldsymbol{X}_h. \tag{7}$$

Note that $\langle G\, q_h, \boldsymbol{v}_h \rangle = \langle \nabla q_h,\, \boldsymbol{v}_h \rangle - \displaystyle\int_{\Gamma_N} q_h\, \boldsymbol{v}_h \cdot \boldsymbol{n}$ and thus, if we consider Dirichlet boundary conditions on all the boundary Γ, the operator G would be the gradient operator.
$\Pi_h^{(k)} : \mathbf{H}^{-1}(\Omega) \mapsto \boldsymbol{X}_h$ defined by

$$(\Pi_h^{(k)}\, \varphi, \boldsymbol{v}_h)_k = \langle \varphi, \boldsymbol{v}_h \rangle, \quad \forall\, \varphi \in \mathbf{H}^{-1}(\Omega),\, \forall \boldsymbol{v}_h \in \boldsymbol{X}_h, \tag{8}$$

for $k=0$ or $k=1$. Observe that from (8) and (7),

$$(\Pi_h^{(k)}(G\,q_h), \boldsymbol{v}_h)_k = -(\nabla\cdot\boldsymbol{v}_h, q_h)_0, \quad \forall q_h \in M_h,\, \forall \boldsymbol{v}_h \in \boldsymbol{X}_h. \tag{9}$$

We then propose to recover the reduced pressure as a solution of the following least-squares minimum residual problem, either with respect to the $\mathbf{L}^2(\Omega)$ or the $\mathbf{H}^1_D(\Omega)$ norms,

$$p_r = \underset{q_r\in M_r}{\operatorname{argmin}}\, J(q_r) := \|\Pi_h^{(k)}\,(G\,q_r - R(\boldsymbol{u}_r))\,\|_k^2, \tag{10}$$

where $R(\boldsymbol{u}_r)\in \mathbf{H}^{-1}(\Omega)$ given by

$$\langle R(\boldsymbol{u}_r), \boldsymbol{v}\rangle = \langle \boldsymbol{f}_r, \boldsymbol{v}\rangle - a(\boldsymbol{u}_r, \boldsymbol{u}_r, \boldsymbol{v}; \mu),\, \forall \boldsymbol{v}\in \mathbf{H}^1_D(\Omega). \tag{11}$$

The optimality conditions of this problem are

$$(\Pi_h^{(k)}\,(G\,p_r), \Pi_h^{(k)}\,(G\,q_r))_k = (\Pi_h^{(k)}\,R(\boldsymbol{u}_r), \Pi_h^{(k)}\,(G\,q_r))_k, \quad \forall\, q_r \in M_r. \tag{12}$$

The following results state that the method is well-defined.

Lemma 1. *Assume that the discrete inf-sup condition* (3) *holds. Then, for* $k=0$ *and* $k=1$,

$$\|q_h\|_{h,k} = \|\Pi_h^{(k)}\,(G\,q_h)\|_k,\, \forall\, q_h \in M_h, \tag{13}$$

is a norm on M_h *which satisfies*

$$\|q_h\|_0 \le \alpha\,\|q_h\|_{h,k},\, \forall\, q_h \in M_h, \tag{14}$$

for some $\alpha>0$. *Moreover, for* $k=1$ *the norm* (13) *is uniformly equivalent to the* $L^2(\Omega)$ *norm on* M_h.

Proof: It is straightforward to prove that $\|\cdot\|_{h,k}$ is a semi-norm on M_h. To prove (14), let $q_h\in M_h$, $q_h\neq 0$. Observe that from (9), the inf-sup condition (3) can be written as

$$\begin{aligned}\beta\,\|q_h\|_0 \le \quad & \sup_{\boldsymbol{v}_h\in\boldsymbol{X}_h} \frac{(\nabla\cdot\boldsymbol{v}_h, q_h)_0}{\|\nabla\boldsymbol{v}_h\|_0} = \sup_{\boldsymbol{v}_h\in\boldsymbol{X}_h} \frac{(\Pi_h^{(k)}\,(G\,q_h), \boldsymbol{v}_h)_k}{\|\nabla\boldsymbol{v}_h\|_0} \\ = \quad & \sup_{\substack{\boldsymbol{v}_h\,\in\,\boldsymbol{X}_h \\ \|\nabla\boldsymbol{v}_h\|_0\,=\,1}} (\Pi_h^{(k)}\,(G\,q_h), \boldsymbol{v}_h)_k = \frac{\|\Pi_h^{(k)}\,(G\,q_h)\|_k^2}{\|\nabla\,\Pi_h^{(k)}\,(G\,q_h)\|_0},\end{aligned} \tag{15}$$

where in the last equality we use that the maximun of the inner product $(\Pi_h^{(k)}\,(G\,q_h), \boldsymbol{v}_h)_k$ is reached when $\boldsymbol{v}_h = \lambda\,\Pi_h^{(k)}\,(G\,q_h)$ for any $\lambda>0$. Then, we obtain the equality with $\hat{\boldsymbol{v}_h} = \dfrac{1}{\|\nabla\,\Pi_h^{(k)}\,(G\,q_h)\|_0}\,\Pi_h^{(k)}\,(G\,q_h)$ such that $\|\nabla\hat{\boldsymbol{v}_h}\|_0 = 1$.

When $k=0$,

$$\frac{\|\Pi_h^{(k)}\,(G\,q_h)\|_k^2}{\|\nabla\,\Pi_h^{(k)}\,(G\,q_h)\|_0} \le c_P\,\|\Pi_h^{(k)}\,(G\,q_h)\|_0 = c_P\,\|q_h\|_{h,0}, \tag{16}$$

where c_P is the Poincaré's constant yielding the inequality $\|\boldsymbol{v}\|_0 \le c_P\,\|\nabla\boldsymbol{v}\|_0,\, \forall\boldsymbol{v}\in\mathbf{H}^1_D(\Omega)$.

When $k=1$,

$$\frac{\|\Pi_h^{(k)}(G\,q_h)\|_1^2}{\|\nabla\,\Pi_h^{(k)}(G\,q_h)\|_0} = \|\Pi_h^{(k)}(G\,q_h)\|_1 = \|q_h\|_{h,1}, \tag{17}$$

Inequality (14) follows from (15), (16) and (17) with $\alpha = \dfrac{M}{\beta}$ being $M = c_P$ for $k=0$ or $M=1$ for $k=1$.

Moreover, from (15) and (17),

$$\|q_h\|_{h,1} = \sup_{\boldsymbol{v}_h \in \boldsymbol{X}_h} \frac{(\nabla\cdot\boldsymbol{v}_h, q_h)}{\|\nabla \boldsymbol{v}_h\|_0} \leq \sqrt{d}\,\|q_h\|_0,$$

which, combined with (14) gives the equivalence of the norms $\|\cdot\|_0$ and $\|\cdot\|_{h,1}$ on M_h. □

Remark 1. *Actually, the equivalence of the norms $\|\cdot\|_0$ and $\|\cdot\|_{h,1}$ on M_h is a re-formulation of the discrete inf-sup property, that states that the $L^2(\Omega)$ norm of the discrete pressures and the $\mathbf{H}^{-1}(\Omega)$ norm of their gradients are equivalent norms in M_h.*

Theorem 3.1. *Assume that the discrete inf-sup condition* (3) *holds. Then problem* (10) *admits a unique solution, which is characterised as the solution of the normal equations* (12).

Proof: Let us consider the space

$$\boldsymbol{S}_r = \{\Pi_h^{(k)}(G\,q_r) \text{ such that } q_r \in M_r\} \subset \boldsymbol{X}_h. \tag{18}$$

Due to the inf-sup condition, the mapping $\mathcal{T} = \Pi_h^{(k)} \circ G : M_r \mapsto \boldsymbol{S}_r$ is bijective. Indeed, it is trivially surjective and from Lemma 1, the inf-sup condition implies that if $\Pi_h^{(k)}(G\,q_r) = 0$, then $q_r = 0$. Therefore, the spaces $\boldsymbol{S}_r$ and M_r are isomorphic. Problem (10) can equivalently be expressed as

$$p_r = \mathcal{T}^{-1}(\boldsymbol{s}_r), \quad \text{with} \quad \boldsymbol{s}_r = \operatorname*{argmin}_{\boldsymbol{\xi}_r \in \boldsymbol{S}_r} \hat{J}(\boldsymbol{\xi}_r) := \|\boldsymbol{\xi}_r - \Pi_h^{(k)}(R(\boldsymbol{u}_r))\|_k^2. \tag{19}$$

Due to the standard theory of least-squares approximation on finite-dimension sub-spaces, this problem admits a unique solution, characterised by the normal equations, that is

$$(\boldsymbol{s}_r, \boldsymbol{\xi}_r)_k = (\Pi_h^{(k)}(R(\boldsymbol{u}_r)), \boldsymbol{\xi}_r)_k, \quad \forall \boldsymbol{\xi}_r \in \boldsymbol{S}_r.$$

These equations indeed are (12). □

3.1 Matrix expression of pressure recovery problem

Let $\{\phi_i\}_{i=1}^{n_h}$ be a basis of $\boldsymbol{X}_h$ and $\{\psi_i\}_{i=1}^{n_r}$ a basis of M_r, then problem (12) is equivalent to

Find $p_r = \displaystyle\sum_{i=1}^{n_r} p_i\,\psi_i \in M_r$ *such that*
$\vec{p} \in \mathbb{R}^{n_r}$ with $(\vec{p})_i = p_i$ is the solution of the linear system:

$$\mathcal{M}\vec{p} = \vec{r} \quad \text{with} \quad \mathcal{M} = \mathcal{B}\,\mathcal{G}^{-1}\,\mathcal{B}^t \text{ and } \vec{r} = \mathcal{B}\,\mathcal{G}^{-1}\,\vec{R}, \tag{20}$$

where

$$\mathcal{B} \in \mathbb{R}^{n_r \times n_h} : \mathcal{B}_{ij} = -(\nabla \cdot \phi_j, \psi_i)_0,$$
$$\mathcal{G} \in \mathbb{R}^{n_h \times n_h} : \mathcal{G}_{ij} = (\phi_j, \phi_i)_k$$
$$\vec{R} \in \mathbb{R}^{n_h} : \vec{R}_i = \langle R(\boldsymbol{u}_r),\, \phi_i \rangle.$$

Indeed, for all $i = 1 \ldots, n_r$,

$$\Pi_h^{(k)}\,(G\,\psi_i) = \sum_{j=1}^{n_h} \alpha_j^i\,\phi_j, \text{ where } \vec{\alpha}^i = \mathcal{G}^{-1}\,\vec{b}^i \text{ with } (\vec{b}^i)_j = -(\nabla \cdot \phi_j, \psi_i).$$

Then,

$$\mathcal{M}_{ij} = (\Pi_h^{(k)}\,(G\,\psi_j),\, \Pi_h^{(k)}\,(G\,\psi_i))_k = (\vec{b}^i)^t\,(\mathcal{G}^{-1})^t\,\vec{b}^j.$$

Note that $\mathcal{M} \in \mathbb{R}^{n_r \times n_r}$ and thus, (20) is a low-dimensional system. Moreover, if we consider the Cholesky factorization of $\mathcal{G}^{-1}$, $\mathcal{G}^{-1} = \mathcal{L}\mathcal{L}^t$, system (20) can be written as

$$\mathcal{D}\,\mathcal{D}^t\,\vec{p} = \mathcal{D}\,\mathcal{L}^t\,\vec{R}, \quad \text{with } \mathcal{D} = \mathcal{B}\mathcal{L}. \tag{21}$$

In this case, $\vec{p} \in \mathbb{R}^{n_r}$ is the solution of problem

$$\vec{p} = \underset{\vec{q} \in \mathbb{R}^{n_r}}{\operatorname{argmin}} \|\mathcal{D}^t\,\vec{q} - \mathcal{L}^t\,\vec{R}\|^2_{\mathbb{R}^{n_r}}. \tag{22}$$

That is, $\vec{p}$ is the least-squares solution of the system $\mathcal{D}^t\,\vec{p} = \mathcal{L}^t\,\vec{R}$. In particular, when the basis of $\boldsymbol{X}_h$ is ortonormal with respect to the inner product $(\cdot,\cdot)_k$, matrix $\mathcal{G} = Id$ and $\vec{p}$ is the least-squares solution of the system $\mathcal{B}^t\vec{p} = \vec{R}$.

From a purely algebraic point of view, the inf-sup condition (3) implies that system (20) admits a unique solution. This is stated as follow

Proposition 1. *Assume that the inf-sup condition* (3) *holds. Then the matrix* $\mathcal{M}$ *of the linear system* (20) *is positive definite and thus, this system admits a unique solution.*

Proof: For simplicity of calculation, let us assume that the basis $\{\phi_i\}_{i=1}^{n_h}$ is orthogonal in $L^2(\Omega)$. Then $\mathcal{G} = Id$ and $\mathcal{M} = \mathcal{B}\,\mathcal{B}^t$. For any $\vec{q} \in \mathbb{R}^{n_r}$,

$$\begin{aligned}\vec{q}^t\mathcal{M}\vec{q} &= \sum_{i,j=1}^{n_r} \vec{q}_i \Big(\sum_{k=1}^{n_h} (\nabla \cdot \phi_k, \psi_i)_0\,(\nabla \cdot \phi_k, \psi_j)_0 \Big) \vec{q}_j \\ &= \sum_{k=1}^{n_h} (\nabla \cdot \phi_k, \sum_{i=1}^{n_r} q_i\,\psi_i)_0\,(\nabla \cdot \phi_k, \sum_{j=1}^{n_r} q_j\,\psi_j)_0 = \sum_{k=1}^{n_h} (\nabla \cdot \phi_k, q_r)_0^2,\end{aligned}$$

with $q_r = \displaystyle\sum_{i=1}^{n_r} q_i\,\psi_i \in M_r$. Then $\vec{q}^t\mathcal{M}\vec{q} \geq 0$, for all $\vec{q} \in \mathbb{R}^{n_r}$. Moreover, $\vec{q}^t\mathcal{M}\vec{q} = 0$ if and only if $(\nabla \cdot \phi_k, q_r)_0$, for all $k = 1 \ldots n_h$ and thus, $(\nabla \cdot \boldsymbol{v}_h, q_r)_0 = 0$ for all $\boldsymbol{v}_h \in \boldsymbol{X}_h$. From (3), this implies that $q_r = 0$ and thus $\vec{q} = 0$. □

4 The pressure gradient supremisers revisited

It is a common practice in ROM of incompressible flows to solve the reduced counterpart of the mixed problem (2) with enriched velocity spaces $\boldsymbol{X}_r$ in such a way that the couple $(\boldsymbol{X}_r, M_r)$ satisfies an inf-sup condition. The reduced velocity space actually is built as

$$\boldsymbol{X}_r = \boldsymbol{S}_r \oplus \boldsymbol{X}_{0r}, \tag{23}$$

where $\boldsymbol{S}_r$ is defined by (18) and $\boldsymbol{X}_{0r}$ is a reduced space formed by weakly divergence-free velocities, that is a subset of $\boldsymbol{X}_{0h}$ given by (5). Observe that the elements of $\boldsymbol{S}_r$ are the pressure-gradient supremisers introduced in [25] and applied in several works to build reduced order models for incompressible flows, for instance [3, 21, 22, 26]. In this way, the reduced problem:

$$\begin{cases} \textit{Find } \boldsymbol{u}_r(\mu) \in \boldsymbol{X}_r \text{ and } p_r(\mu) \in M_r \textit{ such that} \\ a(\boldsymbol{u}_r(\mu), \boldsymbol{u}_r(\mu), \boldsymbol{v}_r; \mu) - (\nabla \cdot \boldsymbol{v}_r, p_r(\mu))_0 = \langle \boldsymbol{f}_r, \boldsymbol{v}_r \rangle, \quad \forall\, \boldsymbol{v}_r \in \boldsymbol{X}_r, \\ (\nabla \cdot \boldsymbol{u}_r(\mu), q_r)_0 = 0, \quad \forall\, q_r \in M_r, \end{cases} \tag{24}$$

is well posed.

The equivalence between this pressure gradient supremizers procedure and the least-squares recovery of the pressure introduced above is stated as follows.

Proposition 2. *Assume that* (23) *holds. Then the velocity* $\boldsymbol{u}_r$ *solution of problem* (24) *satisfies*

$$\begin{cases} \textit{Find } \boldsymbol{u}_r(\mu) \in \boldsymbol{X}_{0r} \textit{ such that} \\ a(\boldsymbol{u}_r(\mu), \boldsymbol{u}_r(\mu), \boldsymbol{v}_{0r}; \mu) = \langle \boldsymbol{f}_r, \boldsymbol{v}_{0r} \rangle, \quad \forall\, \boldsymbol{v}_{0r} \in \boldsymbol{X}_{0r}. \end{cases} \tag{25}$$

and the pressure p_r *satisfies* (12).

Proof: From (23), the velocity $\boldsymbol{u}_r$ is decomposed into

$$\boldsymbol{u}_r = \boldsymbol{s}_r + \boldsymbol{u}_{0r}, \text{ with } \boldsymbol{s}_r \in \boldsymbol{S}_r \text{ and } \boldsymbol{u}_{0r} \in \boldsymbol{X}_{0r}.$$

Let $\pi_r = \mathcal{T}^{-1}(\boldsymbol{s}_r) \in M_r$, that is, $\boldsymbol{s}_r = \Pi_h^{(k)}(G\,\pi_r)$. As $M_r \subset M_h$, $(\nabla \cdot \boldsymbol{u}_{0r}, \pi_r)_0 = 0$. From the second equation in (24), it follows

$$0 = (\nabla \cdot \boldsymbol{u}_r, \pi_r)_0 = (\nabla \cdot \boldsymbol{s}_r, \pi_r)_0 = -(\Pi_h^{(k)}(G\,\pi_r), \boldsymbol{s}_r)_k = -\|\Pi_h^{(k)}(G\,\pi_r)\|_k^2 = -\|\pi_r\|_{h,k}^2.$$

Therefore, $\pi_r = 0$ and consequently $\boldsymbol{s}_r = 0$, what implies $\boldsymbol{u}_r = \boldsymbol{u}_{0r} \in \boldsymbol{X}_{0r}$. Thus, the first equation in (24) gives (25).

Moreover, the first equation in (24) can be written as

$$-(p_r, \nabla \cdot \boldsymbol{v}_r)_0 = \langle R(\boldsymbol{u}_r), \boldsymbol{v}_r \rangle, \quad \forall\, \boldsymbol{v}_r \in \boldsymbol{X}_r,$$

and, from the decomposition (23), this equation is equivalent to

$$-(p_r, \nabla \cdot \boldsymbol{s}_r)_0 = \langle R(\boldsymbol{u}_r), \boldsymbol{s}_r \rangle, \quad \forall\, \boldsymbol{s}_r \in \boldsymbol{S}_r, \tag{26}$$

as $(p_r, \nabla \cdot \boldsymbol{v}_{0r})_0 = 0$, for all $\boldsymbol{v}_{0r} \in \boldsymbol{X}_{0r}$. Then, p_r satisfies

$$(\Pi_h^{(k)}(G\,p_r), \boldsymbol{s}_r)_k = (\Pi_h^{(k)}(R(\boldsymbol{u}_r)), \boldsymbol{s}_r)_k,$$

for all $\boldsymbol{s}_r = \Pi_h^{(k)}(G q_r) \in \boldsymbol{S}_r$ with any $q_r \in M_r$, that is, problem (12). □

Remark 2. *From Proposition 2 the pressure computed by the supremizers procedure is cast as the least-squares pressure provided by the velocity solution of the reduced mixed problem* (24)*. In addition, the computation of this velocity can be partially decoupled from that of the pressure, as it solves problem* (25)*. Therefore the (velocity, pressure) pair provided by the supremizers procedure can be computed by solving two coercive problems, sequentially in two steps. In the first step the velocity is computed by solving* (25) *and in the second step the pressure is computed by solving* (12)*, that is:*

$$\boldsymbol{u}_r \in \boldsymbol{X}_{0r}, \quad a(\boldsymbol{u}_r(\mu), \boldsymbol{u}_r(\mu), \boldsymbol{v}_{0r}; \mu) = \langle \boldsymbol{f}_r, \boldsymbol{v}_{0r} \rangle, \quad \forall\, \boldsymbol{v}_{0r} \in \boldsymbol{X}_{0r};$$

$$p_r \in M_r, \quad (\Pi_h^{(k)}(G\, p_r),\, \Pi_h^{(k)}(G\, q_r))_k = (\Pi_h^{(k)}(R(\boldsymbol{u}_r)), \Pi_h^{(k)}(G\, q_r))_k, \quad \forall\, q_r \in M_r.$$

Remark 3. (26) *is the formulation MER to recover the reduced pressure in ROMs (see [8, 16]). Therefore, Proposition 2 proves that the pressure obtained by this method is equivalent to the pressure given by least-squares method* (10)*.*

Remark 4. *All the preceding theory holds whenever the family of full-order velocity and reduced-order pressure spaces* $(\boldsymbol{X}_h, M_r)$ *satisfies the discrete inf-sup condition. Then,* $\boldsymbol{X}_h$ *needs not to be the full finite element space appearing in the FOM problem* (4)*, but it can be replaced by any smaller space that ensures the inf-sup condition. For instance, it can be a reduced space containing non-weakly divergence free velocities, or a finite element space in a coarse grid. This would decrease the time needed to compute in the off-line step the matrix* $\mathcal{G}^{-1}$ *appearing in* (20)*, without increasing the error in the computation of* p_r *(see Theorem 5.1 below).*

Remark 5. *The previous analysis leads to casting general mixed methods in terms of pressure gradient supremisers. More specifically, if a pair of discrete velocity-pressure spaces* $(\boldsymbol{X}_h, M_h) \subset \mathbf{H}_D^1(\Omega) \times L_0^2(\Omega)$ *satisfies the inf-sup condition* (3) *then* $\boldsymbol{X}_h$ *can be expressed as*

$$\boldsymbol{X}_h = \boldsymbol{S}_h \oplus \boldsymbol{X}_{0h}, \text{ with } \boldsymbol{S}_h = \{\Pi_h^{(k)}(G\, q_h) \text{ such that } q_h \in M_h\}, \tag{27}$$

for either $k = 0$ *or* $k = 1$*.*

Indeed, for any $\boldsymbol{x}_h \in \boldsymbol{X}_h$*, because of the inf-sup condition, there exists a unique* $(\boldsymbol{x}_{0h}, \pi_h) \in \boldsymbol{X}_h \times M_h$ *solution of problem*

$$\begin{cases} (\boldsymbol{x}_{0h}, \boldsymbol{v}_h)_k - (\nabla \cdot \boldsymbol{v}_h, \pi_h)_0 = (\boldsymbol{x}_h, \boldsymbol{v}_h)_k, & \forall\, \boldsymbol{v}_h \in \boldsymbol{X}_h, \\ (\nabla \cdot \boldsymbol{x}_{0h}, q_h)_0 = 0, & \forall\, q_h \in M_h, \end{cases}$$

for $k = 0$ *or* $k = 1$*. Then,* $\boldsymbol{s}_h = \boldsymbol{x}_h - \boldsymbol{x}_{0h}$ *verifies*

$$(\boldsymbol{s}_h, \boldsymbol{v}_h)_k = -(\nabla \cdot \boldsymbol{v}_h, \pi_h)_0 = (\Pi_h^{(k)}(G\, \pi_h),\, \boldsymbol{v}_h)_k, \quad \forall\, \boldsymbol{v}_h \in \boldsymbol{X}_h.$$

Therefore, $\boldsymbol{s}_h = \Pi_h^{(k)}(G\, \pi_h) \in \boldsymbol{S}_h$*. The sum is direct because if* $\boldsymbol{x}_h \in \boldsymbol{S}_h \cap \boldsymbol{X}_{0h}$ *then* $\boldsymbol{x}_h = 0$ *as occurs to* $\boldsymbol{s}_r$ *in Proposition 2.*

Moreover, π_h *is the solution of problem*

$$(\Pi_h^{(k)}(G\, \pi_h),\, \Pi_h^{(k)}(G\, q_h))_k = (\Pi_h^{(k)}(\boldsymbol{x}_h - \boldsymbol{x}_{0h}),\, \Pi_h^{(k)}(G\, q_h))_k, \quad \forall\, q_h \in M_h,$$

and thus, π_h *is the least-squares pressure recovered by* (10) *on* M_h *instead* M_r *with* $R(\boldsymbol{x}_h) = \boldsymbol{x}_h - \boldsymbol{x}_{0h}$*.*

5 Error estimates

In this section we obtain optimal error estimates for the pressure in terms of the approximation properties of space M_r and the distance between the FOM and ROM velocities. For that, let us assume that an inverse inequality between the $\mathbf{L}^2(\Omega)$ and $\mathbf{H}^1_0(\Omega)$ semi-norms holds on space $\boldsymbol{X}_h$:

$$\|\nabla \boldsymbol{v}_h\|_0 \leq C_h \, \|\boldsymbol{v}_h\|_0, \quad \forall \, \boldsymbol{v}_h \in \boldsymbol{X}_h, \tag{28}$$

where $C_h > 0$ is unbounded as the discretisation parameter h decreases to zero. This constant depends on the actual kind of discretisation used. For instance, for finite element discretisations this constant scales as $h_{\min}^{-1}$, where $h_{\min}$ is the smallest diameter of the grid elements.

In sequel, we will use the following notation: given a Banach space X endowed with the norm $\|\cdot\|_X$ and a subset $Y \subset X$, we denote the distance from an element $x \in X$ to Y by

$$d_X(x, Y) = \inf_{\zeta \in Y} \|x - \zeta\|_X.$$

Theorem 5.1. *Assume that the discrete inf-sup condition* (3) *holds, then the solution of problem* (12) *satisfies the following error estimates:*

If $k = 0$,

$$\|p_h - p_r\|_0 \leq C_h \left(d_{L^2(\Omega)}(p_h, M_r) + \|R(\boldsymbol{u}_h) - R(\boldsymbol{u}_r)\|_{\mathbf{H}^{-1}(\Omega)} \right), \tag{29}$$

where C_h *is given by* (28).

If $k = 1$,

$$\|p_h - p_r\|_0 \leq C \left(d_{L^2(\Omega)}(p_h, M_r) + \|R(\boldsymbol{u}_h) - R(\boldsymbol{u}_r)\|_{\mathbf{H}^{-1}(\Omega)} \right), \tag{30}$$

where C *is a positive constant independent of* h.

Here $(\boldsymbol{u}_h, p_h)$ *is a solution of the FOM problem* (4), $R(\boldsymbol{u}_r)$ *is defined by* (11) *and similarly,* $\langle R(\boldsymbol{u}_h), \boldsymbol{v} \rangle = \langle \boldsymbol{f}_h, \boldsymbol{v} \rangle - a(\boldsymbol{u}_h, \boldsymbol{u}_h, \boldsymbol{v}; \mu)$, $\forall \boldsymbol{v} \in \mathbf{H}^1_D(\Omega)$.

Proof: From (4) it holds

$$(\Pi_h^{(k)}(G\, p_h), \boldsymbol{v}_h)_k = (\Pi_h^{(k)}(R(\boldsymbol{u}_h)), \boldsymbol{v}_h)_k, \text{ for any } \boldsymbol{v}_h \in \boldsymbol{X}_h.$$

Let $\hat{p}_r$ be the $L^2(\Omega)$ proyection of p_h on M_r. It holds

$$(\Pi_h^{(k)}\,(G\,\hat{p}_r),\, \Pi_h^{(k)}\,(G\,q_r))_k = (\Pi_h^{(k)}\,G\,(\hat{p}_r - p_h) + (\Pi_h^{(k)}(R(\boldsymbol{u}_h)),\, \Pi_h^{(k)}\,(G\,q_r))_k, \quad \forall\, q_r \in M_r.$$

Let us define the error $e_r = \hat{p}_r - p_r \in M_r$ and subtract (12) from this last equality. We deduce the following equation for e_r:

$$\begin{aligned} (\Pi_h^{(k)}\,(G\,e_r),\, \Pi_h^{(k)}\,(G\,q_r))_k \;&= (\Pi_h^{(k)}\,G\,(\hat{p}_r - p_h),\, \Pi_h^{(k)}\,(G\,q_r))_k \\ &\quad + (\Pi_h^{(k)}\,(R(\boldsymbol{u}_h) - R(\boldsymbol{u}_r)),\, \Pi_h^{(k)}\,(G\,q_r))_k, \quad \forall\, q_r \in M_r. \end{aligned} \tag{31}$$

Taking $q_r = e_r$,

$$\begin{aligned} &\|\Pi_h^{(k)}\,(G\,e_r)\|_k^2 \\ &\quad = (\Pi_h^{(k)}\,\nabla(\hat{p}_r - p_h),\, \Pi_h^{(k)}\,(G\,e_r))_k + (\Pi_h^{(k)}\,(R(\boldsymbol{u}_h) - R(\boldsymbol{u}_r)),\, \Pi_h^{(k)}\,(G\,e_r))_k. \end{aligned} \tag{32}$$

We now bound the terms of the last line of (32):

$$\begin{aligned}(\Pi_h^{(k)}\,\nabla(\hat{p}_r - p_h),\,\Pi_h^{(k)}\,(G\,e_r))_k &= -(\nabla\cdot\Pi_h^{(k)}\,(G\,e_r),\hat{p}_r - p_h)_0\\ &\leq \sqrt{d}\,\|\nabla\,\Pi_h^{(k)}\,(G\,e_r)\|_0\,\|\hat{p}_r - p_h\|_0.\end{aligned} \tag{33}$$

$$\begin{aligned}(\Pi_h^{(k)}\,(R(\boldsymbol{u}_h) - R(\boldsymbol{u}_r)),\,\Pi_h^{(k)}\,(G\,e_r))_k &= \langle R(\boldsymbol{u}_h) - R(\boldsymbol{u}_r),\Pi_h^{(k)}\,(G\,e_r)\rangle\\ &\leq \|R(\boldsymbol{u}_h) - R(\boldsymbol{u}_r)\|_{\mathbf{H}^{-1}(\Omega)}\,\|\nabla\,\Pi_h^{(k)}\,(G\,e_r)\|_0.\end{aligned} \tag{34}$$

Then, from estimates (32), (33) and (34) we have:

If $k=0$, applying (28) to $\|\nabla\,\Pi_h^{(k)}\,(G\,e_r)\|_0$,

$$\|e_r\|_{h,0} \leq C_h\Big(\sqrt{d}\,\|\hat{p}_r - p_h\|_0 + \|R(\boldsymbol{u}_h) - R(\boldsymbol{u}_r)\|_{\mathbf{H}^{-1}(\Omega)}\Big), \tag{35}$$

If $k=1$,

$$\|e_r\|_{h,1} \leq \sqrt{d}\,\|\hat{p}_r - p_h\|_0 + \|R(\boldsymbol{u}_h) - R(\boldsymbol{u}_r)\|_{\mathbf{H}^{-1}(\Omega)}. \tag{36}$$

Estimate (29) and (30) follow from estimates (35), (36) and (14). □

5.1 Error estimates for the evolutionary model

In this section we apply the previous analysis to the evolutionary incompressible Navier-Stokes equation. That is, assuming that the flow takes place during a time interval $[0,T]$, we consider the problem:

Find a velocity field $\boldsymbol{u}(\mu):\Omega\times(0,T)\to\mathbb{R}^d$ *and a pressure* $p(\mu):\Omega\times(0,T)\to\mathbb{R}$ *such that*

$$\begin{cases}\partial_t\,\boldsymbol{u}(\mu) + \boldsymbol{u}(\mu)\cdot\nabla\boldsymbol{u}(\mu) - \mu\Delta\boldsymbol{u}(\mu) + \nabla p(\mu) = \boldsymbol{f} & \text{in } \Omega\times(0,T),\\ \nabla\cdot\boldsymbol{u}(\mu) = 0 & \text{in } \Omega\times(0,T),\\ \boldsymbol{u}(\mu) = 0 & \text{on } \Gamma_D\times(0,T),\\ -\mu\,\nabla\boldsymbol{u}(\mu)\cdot\boldsymbol{n} + p(\mu)\boldsymbol{n} = 0 & \text{on } \Gamma_N\times(0,T),\\ \boldsymbol{u}(\mu,0) = \boldsymbol{u}_0, & \text{in } \Omega,\end{cases} \tag{37}$$

where $\boldsymbol{u}_0$ is a initial field velocity given.

Consider a uniform partition of the interval $[0,T]$, $\{0=t_0<t_1<\ldots t_N=T\}$, with time-step size $\Delta t = T/N$. The time discretization of problem (37) by the Backward Euler scheme carries to the following family of stationary problems:

Given the initialization $\boldsymbol{u}^0(\mu) = u_0$,

$$\begin{cases}\text{Find } \boldsymbol{u}^n(\mu)\in\mathbf{H}^1_D(\Omega) \text{ and } p^n(\mu)\in L^2_0(\Omega) \text{ such that}\\ a(\boldsymbol{u}^n(\mu),\boldsymbol{u}^n(\mu),\boldsymbol{v};\mu) - (\nabla\cdot\boldsymbol{v},p^n(\mu))_0 = \langle\boldsymbol{f}^n,\boldsymbol{v}\rangle, \quad \forall\,\boldsymbol{v}\in\mathbf{H}^1_D(\Omega),\\ (\nabla\cdot\boldsymbol{u}^n(\mu),q)_0 = 0 \quad \forall\,q\in L^2_0(\Omega),\\ \forall\,n=1,2,\ldots N.\end{cases} \tag{38}$$

For each time step, this problem fits into the formulation (2) with $\gamma = \frac{1}{\Delta t}$ and $\boldsymbol{f}^n = \boldsymbol{f} + \frac{1}{\Delta t}\boldsymbol{u}^{n-1}$. Then, we obtain time-space aproximations of a solution of problem (37) applying the FOM (4) to problem (38): $(\boldsymbol{u}_h^n(\mu), p_h^n(\mu)) \in \boldsymbol{X}_h \times M_h$ such that

$$\begin{cases} a(\boldsymbol{u}_h^n(\mu), \boldsymbol{u}_h^n(\mu), \boldsymbol{v}_h; \mu) - (\nabla \cdot \boldsymbol{v}_h, p_h^n(\mu))_0 = \langle \boldsymbol{f}_h^{n-1}, \boldsymbol{v}_h \rangle, \quad \forall\, \boldsymbol{v}_h \in \boldsymbol{X}_h, \\ (\nabla \cdot \boldsymbol{u}_h^n(\mu), q_h)_0 = 0 \quad \forall\, q_h \in M_h, \end{cases} \tag{39}$$

where $\boldsymbol{f}_h^{n-1} = \boldsymbol{f} + \frac{1}{\Delta t}\boldsymbol{u}_h^{n-1}$.
We also obtain ROM aproximations: $(\boldsymbol{u}_r^n(\mu), p_r^n(\mu)) \in \boldsymbol{X}_r \times M_r$, where the reduced velocity $\boldsymbol{u}_r^n(\mu)$ is computed by problem

$$a(\boldsymbol{u}_r^n(\mu), \boldsymbol{u}_r^n(\mu), \boldsymbol{v}_r; \mu) = \langle \boldsymbol{f}_r^{n-1}, \boldsymbol{v}_r \rangle, \quad \forall\, \boldsymbol{v}_r \in \boldsymbol{X}_r, \tag{40}$$

where $\boldsymbol{f}_r^{n-1} = \boldsymbol{f} + \frac{1}{\Delta t}\boldsymbol{u}_r^{n-1}$, and the reduced pressure $p_r^n(\mu)$ is recovered from the reduced velocity by the least-squares method (10).

To obtain error estimates for the reduced pressure we introduce the following discrete functions. In the following we omit the dependency on the parameters for brevity.

- $\boldsymbol{u}_h : [0,T] \to \boldsymbol{X}_h$ is the piecewise linear in time function such that $\boldsymbol{u}_h(t_n) = \boldsymbol{u}_h^n$.
- $p_h : [0,T] \to M_h$ is the piecewise constant in time function that takes the value p_h^n on (t_{n-1}, t_n).
- $\boldsymbol{u}_r : [0,T] \to \boldsymbol{X}_r$ is the piecewise linear in time function such that $\boldsymbol{u}_r(t_n) = \boldsymbol{u}_r^n$.
- $p_r : [0,T] \to M_r$ is the piecewise constant in time function that takes the value p_r^n on (t_{n-1}, t_n).

Theorem 5.2. *Assume that the discrete inf-sup condition* (3) *holds, then the least-squares reduced pressure for problem* (37) *satisfies the following error estimates:*

If $k = 0$,

$$\|p_h - p_r\|_{L^1(L^2(\Omega))} \leq C_h \left(d_{L^1(L^2(\Omega))}(p_h, M_r) + \|\boldsymbol{u}_h - \boldsymbol{u}_r\|_{L^2(\mathbf{H}^1_D(\Omega))} \right), \tag{41}$$

where C_h *is given by* (28).

If $k = 1$,

$$\begin{aligned} \|p_h - p_r\|_{L^1(L^2(\Omega)} \;\leq\; & C \Big(d_{L^1(L^2(\Omega))}(p_h, M_r) + \\ & \|\boldsymbol{u}_h - \boldsymbol{u}_r\|_{L^2(\mathbf{H}^1_D(\Omega))} + \|D_t(\boldsymbol{u}_h - \boldsymbol{u}_r)\|_{L^1(\mathbf{H}^{-1}(\Omega))} \Big), \end{aligned} \tag{42}$$

where C *is a positive constant independent of* h *and* $D_t\boldsymbol{v} = \frac{1}{\Delta t}(\boldsymbol{v}(t_n) - \boldsymbol{v}(t_{n-1}))$ *denote the discrete time derivate.*

Proof: We obtain estimates for the errors $\|p_h^n - p_r^n\|_0$ from Theorem 5.1. Here, we firstly observe that

$$R(\boldsymbol{u}_h^n) - R(\boldsymbol{u}_r^n) = A(\boldsymbol{u}_r^n) - A(\boldsymbol{u}_h^n),$$

where

$$\langle A(\boldsymbol{w}), \boldsymbol{v} \rangle = \langle D_t \boldsymbol{w}, \boldsymbol{v} \rangle + \langle \boldsymbol{w} \cdot \nabla \boldsymbol{w}, \boldsymbol{v} \rangle - \mu\, (\nabla \boldsymbol{w}, \nabla \boldsymbol{v})_0, \quad \forall\, \boldsymbol{w}, \boldsymbol{v} \in \mathbf{H}^1_D(\Omega).$$

Moreover, depending on the value of k, one of the terms of the residual in the last term of (32) disappears. Indeed, the operator Π_h^0 restricted to $\boldsymbol{L}^2(\Omega)$ coincides with the $\boldsymbol{L}^2$ the orthogonal projection

operator on $\boldsymbol{X}_h$. Consequently, when $k=0$ there is no contribution from the discrete time derivative term of the residual to the error:

$$\begin{aligned}(\Pi_h^{(0)}\,(D_t(\boldsymbol{u}_h^n-\boldsymbol{u}_r^n)),\,\Pi_h^{(0)}\,(G\,e_r^n))_0 &= (D_t(\boldsymbol{u}_h^n-\boldsymbol{u}_r^n),\,\Pi_h^{(0)}\,(G\,e_r^n))_0\\ &= -(\nabla\cdot(D_t(\boldsymbol{u}_h^n-\boldsymbol{u}_r^n)),e_r^n)_0=0.\end{aligned}$$

Likewise, when $k=1$ there is no contribution of the diffusive term of the residual to the error:

$$(\Pi_h^{(1)}\,(\boldsymbol{u}_h^n-\boldsymbol{u}_r^n),\,\Pi_h^{(1)}\,(G\,e_r^n))_1=(\boldsymbol{u}_h^n-\boldsymbol{u}_r^n,\,\Pi_h^{(1)}\,(G\,e_r^n))_1=-(\nabla\cdot(\boldsymbol{u}_h^n-\boldsymbol{u}_r^n),e_r^n)_0=0.$$

Then, from the estimates given by Theorem 5.1 for $\|p_h^n-p_r^n\|_0$, multiplying by Δt and adding up over n, we obtain:
If $k=0$,

$$\sum_{n=1}^{N}\Delta t\,\|p_h^n-p_r^n\|_0\le C_h\sum_{n=1}^{N}\Delta t\Big(d_{L^2(\Omega)}(p_h^n,M_r)+\|A^{(0)}(\boldsymbol{u}_h^n)-A^{(0)}(\boldsymbol{u}_r^n)\|_{\mathbf{H}^{-1}(\Omega)}\Big).\tag{43}$$

If $k=1$,

$$\sum_{n=1}^{N}\Delta t\,\|p_h^n-p_r^n\|_0\le C\sum_{n=1}^{N}\Delta t\,\Big(d_{L^2(\Omega)}(p_h^n,M_r)+\|A^{(1)}(\boldsymbol{u}_h^n)-A^{(1)}(\boldsymbol{u}_r^n)\|_{\mathbf{H}^{-1}(\Omega)}\Big),\tag{44}$$

where

$$\begin{aligned}\langle A^{(0)}\,\boldsymbol{w},\boldsymbol{v}\rangle&=(\boldsymbol{w}\cdot\nabla\boldsymbol{w},\boldsymbol{v})_0+\mu\,(\nabla\boldsymbol{w},\nabla\boldsymbol{v})_0,\\ \langle A^{(1)}\,\boldsymbol{w},\boldsymbol{v}\rangle&=(D_t\,\boldsymbol{w},\boldsymbol{v})_0+(\boldsymbol{w}\cdot\nabla\boldsymbol{w},\boldsymbol{v})_0,\quad\forall\,\boldsymbol{w},\boldsymbol{v}\in\mathbf{H}_D^1(\Omega).\end{aligned}$$

We now bound $\displaystyle\sum_{n=1}^{N}\Delta t\,\|A^{(k)}(\boldsymbol{u}_h^n)-A^{(k)}(\boldsymbol{u}_r^n)\|_{\mathbf{H}^{-1}(\Omega)}$. For the convective term, we have:

$$\begin{aligned}(\boldsymbol{u}_h^n\cdot\nabla\boldsymbol{u}_h^n-\boldsymbol{u}_r^n\cdot\nabla\boldsymbol{u}_r^n,\,\boldsymbol{v})_0&\le C\,\big(\|\boldsymbol{u}_h^n-\boldsymbol{u}_r^n\|_{0,3}\,\|\nabla\boldsymbol{u}_h^n\|_0+\|\boldsymbol{u}_r^n\|_{0,3}\,\|\nabla(\boldsymbol{u}_h^n-\boldsymbol{u}_r^n)\|_0\big)\,\|\boldsymbol{v}\|_{0,6},\\ &\le C\,\big(\|\boldsymbol{u}_h^n-\boldsymbol{u}_r^n\|_1\,\|\boldsymbol{u}_h^n\|_1+\|\boldsymbol{u}_r^n\|_1\,\|\boldsymbol{u}_h^n-\boldsymbol{u}_r^n\|_1\big)\,\|\nabla\boldsymbol{v}\|_0,\end{aligned}$$

where we denote by $\|\cdot\|_{k,p}$ the norm in $W^{k,p}(\Omega)^d$ and we have using HÃlder's inequality and Sobolev's embedding from $\mathbf{H}_D^1(\Omega)$ in $\boldsymbol{L}^3(\Omega)$ and $\boldsymbol{L}^6(\Omega)$. From here, we get

$$\begin{aligned}&\sum_{n=1}^{N}\Delta t\,\|\boldsymbol{u}_h^n\cdot\nabla\boldsymbol{u}_h^n-\boldsymbol{u}_r^n\cdot\nabla\boldsymbol{u}_r^n\|_{\mathbf{H}^{-1}(\Omega)}\\ &\quad\le C\,\Big(\sum_{n=1}^{N}\Delta t\,\|\boldsymbol{u}_h^n-\boldsymbol{u}_r^n\|_1^2\Big)^{1/2}\Big[\Big(\sum_{n=1}^{N}\Delta t\,\|\boldsymbol{u}_h^n\|_1^2\Big)^{1/2}+\Big(\sum_{n=1}^{N}\Delta t\,\|\boldsymbol{u}_r^n\|_1^2\Big)^{1/2}\Big]\\ &\quad=C\,\|\boldsymbol{u}_h-\boldsymbol{u}_r\|_{L^2(\mathbf{H}_D^1(\Omega))}\Big[\|\boldsymbol{u}_h\|_{L^2(\mathbf{H}_D^1(\Omega))}+\|\boldsymbol{u}_r\|_{L^2(\mathbf{H}_D^1(\Omega))}\Big],\end{aligned}$$

using Young's inequality. Thus,

$$\sum_{n=1}^{N}\Delta t\,\|\boldsymbol{u}_h^n\cdot\nabla\boldsymbol{u}_h^n-\boldsymbol{u}_r^n\cdot\nabla\boldsymbol{u}_r^n\|_{\mathbf{H}^{-1}(\Omega)}\le C\,\|\boldsymbol{u}_h-\boldsymbol{u}_r\|_{L^2(\mathbf{H}_D^1(\Omega))},\tag{45}$$

as the solutions of the FOM and ROM methods are uniformly bounded in $\mathbf{H}^1_D(\Omega)$.
For the diffusive term:

$$\begin{aligned} \mu \sum_{n=1}^{N} \Delta t \, (\nabla(\boldsymbol{u}_h^n - \boldsymbol{u}_r^n), \, \nabla \boldsymbol{v})_0 \quad &\leq \mu \, \|\nabla \boldsymbol{v}\|_0 \sum_{n=1}^{N} \Delta t \, \|\nabla(\boldsymbol{u}_h^n - \boldsymbol{u}_r^n)\|_0 \\ &= \mu \, \|\nabla \boldsymbol{v}\|_0 \, \|\boldsymbol{u}_h^n - \boldsymbol{u}_r^n\|_{L^1(\mathbf{H}^1_D(\Omega))}. \end{aligned} \tag{46}$$

For the discrete time derivate term:

$$\begin{aligned} \sum_{n=1}^{N} \Delta t \, (D_t(\boldsymbol{u}_h^n - \boldsymbol{u}_r^n), \, \boldsymbol{v})_0 \quad &\leq \quad \sum_{n=1}^{N} \Delta t \, \|D_t(\boldsymbol{u}_h^n - \boldsymbol{u}_r^n)\|_{\mathbf{H}^{-1}(\Omega)} \, \|\nabla \boldsymbol{v}\|_0 \\ &= \quad \|D_t(\boldsymbol{u}_h - \boldsymbol{u}_r)\|_{L^1(\mathbf{H}^{-1}(\Omega))} \, \|\nabla \boldsymbol{v}\|_0. \end{aligned} \tag{47}$$

Then, in (43)

$$\sum_{n=1}^{N} \Delta t \, \|A^{(0)}(\boldsymbol{u}_h^n) - A^{(0)}(\boldsymbol{u}_r^n)\|_{\mathbf{H}^{-1}(\Omega)} \leq C \, \|\boldsymbol{u}_h - \boldsymbol{u}_r\|_{L^2(\mathbf{H}^1_D(\Omega))},$$

from (45) and (46), and we obtain (41). Likewise, in (44)

$$\sum_{n=1}^{N} \Delta t \, \|A^{(1)}(\boldsymbol{u}_h^n) - A^{(1)}(\boldsymbol{u}_r^n)\|_{\mathbf{H}^{-1}(\Omega)} \leq C \, \|\boldsymbol{u}_h - \boldsymbol{u}_r\|_{L^2(\mathbf{H}^1_D(\Omega))} + \|D_t(\boldsymbol{u}_h - \boldsymbol{u}_r)\|_{L^1(\mathbf{H}^{-1}(\Omega))},$$

from (45) and (47), and we obtain (42). □

6 Numerical results

In the following, we perform numerical tests to assess and quantify the error estimates derived in the previous section for the pressure obtained by the least-squares procedure for $k = 0$ and $k = 1$ and compare the results with those obtained by the method introduced by Chacon et al (see [6]). In this reference the authors allow the solution of the pressure equation by duality of the momentum conservation equation with gradients of the reduced pressure basis functions. This method is introduced from a minimum residual projection approach and consists in solving a Poisson equation for the pressure, but with the advantage of setting the right boundary conditions and thus ensuring a better accuracy in its recovery. Note that in this validation section, we limit ourselves to the calculation of the pressure that is the subject of the paper.

However, before proceeding to the numerical experiments, we address a crucial issue concerning the calculation of the small amplitude POD modes. These, if poorly evaluated, can pollute the approximation.

6.1 Treatment of small amplitude modes

In the following we address the stability issue that may arise in the least-squares pressure ROM (LSpROM) due to small amplitude modes. These modes are susceptible to bring numerical noise to the computed solutions as they are most likely to cause loss of orthogonality and consequently amplification of the errors. To prevent this from happening, we propose two variants of the LSpROM problem by tuning the optimization process to ensure bounds on the amplitudes of the predicted solutions.

LSpROM(1) : Inequality bound constraint A way to limit the error amplification in the LSpROM is by constraining the problem at each time step. This procedure suggests to enforce a bound on the amplitudes of the computed modes such that $p_j^2 \leq \varepsilon\lambda_j$ with $\{\lambda_j\}_1^{n_r}$ the pressure POD eigenvalues and ε a small threshold chosen by the user. As a result, instead of solving the unconstrained LSpROM problem (22) in $\mathbb{R}^{n_r}$, we seek the latent variable $\vec{p}$ in a smaller space as the solution to the constrained problem

$$\vec{p} = \underset{\vec{q}\in\mathbb{R}^{n_r} \text{ s.t } q_j^2\leq\varepsilon\lambda_j}{\operatorname{argmin}} \|\mathcal{D}^t\,\vec{q} - \mathcal{L}^t\,\vec{R}\|^2_{\mathbb{R}^{n_r}}. \tag{48}$$

In this case, the reduced pressure is solved by using the projected descent gradient method.

LSpROM(2) : Orthogonality constraint In this approach, rather than tuning the low amplitude modes bound through the threshold ϵ, we suggest to compute the pressure ROM in one shot for all the sampling time steps, by enforcing orthogonality constraints on the normalized modes.

Let $[\lambda] = \operatorname{diag}(\{\lambda_1, \ldots, \lambda_{n_r}\}) \in \mathbb{R}^{n_r\times n_r}$ be the diagonal matrix of pressure POD eigenvalues, $[\vec{q_*}] = [\vec{q_*}^1 \ \ldots \ \vec{q_*}^N] \in \mathbb{R}^{n_r\times N}$ the matrix carrying the orthonormalized temporal modes such that $[\vec{q_*}][\vec{q_*}]^t = I_{n_r}$, and $[\vec{R}] = [\vec{R}^1 \ \ldots \ \vec{R}^N] \in \mathbb{R}^{n_h\times N}$ the matrix formed by concatenating the LSpROM residuals. The orthogonality constrained LSpROM problem reads as follows

$$[\vec{p_*}] = \underset{[\vec{q_*}][\vec{q_*}]^t=I_{n_r}}{\operatorname{argmin}} \|\mathcal{D}^t\,[\lambda]\,[\vec{q_*}] - \mathcal{L}^t\,[\vec{R}]\|^2_F, \tag{49}$$

where $||\cdot||_F$ denotes the Frobenius norm. The above problem is formulated as

$$\min_{[\vec{q_*}]\in\mathbb{R}^{n_r\times N}} \max_{[\eta]\in\mathbb{R}^{n_r\times n_r}} \mathscr{L}_2([\vec{q_*}],[\eta]),$$

where $[\eta]$ stands for the Lagrange multiplier symmetric matrix and $\mathscr{L}_2$ the Lagrange functional given by

$$\mathscr{L}_2([\vec{q_*}],[\eta]) = \|\mathcal{D}^t\,[\lambda]\,[\vec{q_*}] - \mathcal{L}^t\,[\vec{R}]\|^2_F + < [\eta], [\vec{q_*}][\vec{q_*}]^t - I_{n_r} >_F .$$

The differentiation of the Lagrangian function gives

$$\begin{aligned}
\frac{\partial\mathscr{L}_2}{\partial[\vec{q_*}]}([\vec{p_*}],[\eta]) &= \left(2\,[\lambda]\,\mathcal{D}\,\mathcal{D}^t\,[\lambda] + [\eta]\right)\,[\vec{p_*}] - 2\,[\lambda]\,\mathcal{D}\,\mathcal{L}^t\,[\vec{R}] \\
\frac{\partial\mathscr{L}_2}{\partial[\eta]}([\vec{p}],[\eta]) &= [\vec{p_*}][\vec{p_*}]^t - I_{n_r}
\end{aligned}$$

By canceling the first derivative equation, we obtain

$$\left(2\,[\lambda]\,\mathcal{D}\,\mathcal{D}^t\,[\lambda] + [\eta]\right)\,[\vec{p_*}] = 2\,[\lambda]\,\mathcal{D}\,\mathcal{L}^t\,[\vec{R}].$$

Let U, Σ, V be the SVD components of the matrix $[\vec{R}]^t\,\mathcal{L}\,\mathcal{D}^t\,[\lambda]$ such that

$$[\vec{R}]^t\,\mathcal{L}\,\mathcal{D}^t\,[\lambda] = U\,\Sigma\,V^t.$$

It follows by using the orthogonality constraint equations, that

$$\left(2\,[\lambda]\,\mathcal{D}\,\mathcal{D}^t\,[\lambda] + [\eta]\right) = 2\,V\,\Sigma\,V^t,$$

which yields

$$[\vec{p_*}] = V\, U^t.$$

Finally, the predicted least-squares pressure with the right POD amplitudes is recovered as $[\vec{p}] = [\lambda]\,[\vec{p_*}]$. In what follows, we quantify the errors of the LSpROM obtained by the three approaches, the unconstrained approach (22), the constrained approach with inequalities (48) where we chose $\varepsilon = 5 \cdot 10^{-3}$, and the constrained approach with orthogonality (49). The errors for the LSpROM are calculated by varying simultaneously the POD truncation order of velocity and pressure.

6.2 Description of the test cases

The data used for the construction of the POD subspaces are obtained by using Fenics [18] with Taylor-Hood element $\mathbb{P}_2/\mathbb{P}_1$. To quantify the pressure error estimates derived in the previous section, we consider two classical benchmark numerical examples, the flow past a cylinder at $Re = 100$ and the lid-driven cavity flow at $Re = 10000$

Flow past a cylinder Re = 100.

The flow is considered in a channel of rectangular shape with height $H = 30D$ and length $45D$, with a cylinder of diameter D placed at $L_1 = 10D$ from the left boundary and $H/2$ from the bottom wall. At the entrance of the channel, a horizontal velocity of magnitude U is imposed. On the remaining boundaries, we set a free-slip condition on the horizontal walls, a no-slip condition on the cylinder, and a normal stress free condition on the right boundary to allow the fluid to exit through the outlet of the channel. Regarding the computational aspects, we use a space-time discretizations consisting of a non-uniform triangular mesh made of 21174 cells, and a first order semi-implicit Euler integration scheme of step $\Delta t = 10^{-2}$. The resulting flow shows a creation of alternating low-high pressure vortices downstream the cylinder, triggering the generation of periodic Von Karman vortex pattern in the wake region. These structures are illustrated in Figure 1.

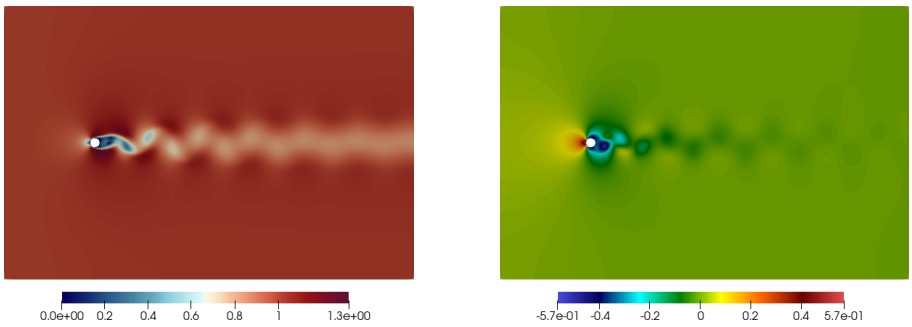

(a) Velocity (b) Pressure

Figure 1: High fidelity velocity and pressure solutions of the flow past a cylinder, $Re = 100$

In order to construct the velocity and pressure POD bases, 200 uniformly distributed snapshots covering 8 periods of the periodic regime of the flow are considered.

Results and discussion From the top left subfigures of Figures 2, we can already see that the eigenvalues of the POD corresponding to the pressure decrease exponentially to zero. This means that the few first modes carry the most of the flow energy and thus, are capable of reproducing the

dynamics with a very good accuracy. The top right subfigures of Figures 2 shows that, using LSpROM after a certain number of modes, the pressure errors start to increase, in contrast to what is expected by the theory. Our analysis of this result led us to understand that this behaviour occurs when the POD modes are no longer numerically orthogonal. Precisely, this occurs for very small eigenvalues. To prevent this unwanted numerical defect, we proposed to couple the pressure calculation using LSpROM with one of the two constrained approaches described in subsection 6.1. We then observe a control of the error in the region where the growth was initially observed. In particular, the obvious improvement takes place for the constrained LSpROM(2), that provides a nearly monotonic decrease of errors as the number of POD modes increases (see the bottom right subfigures of Figures 2).

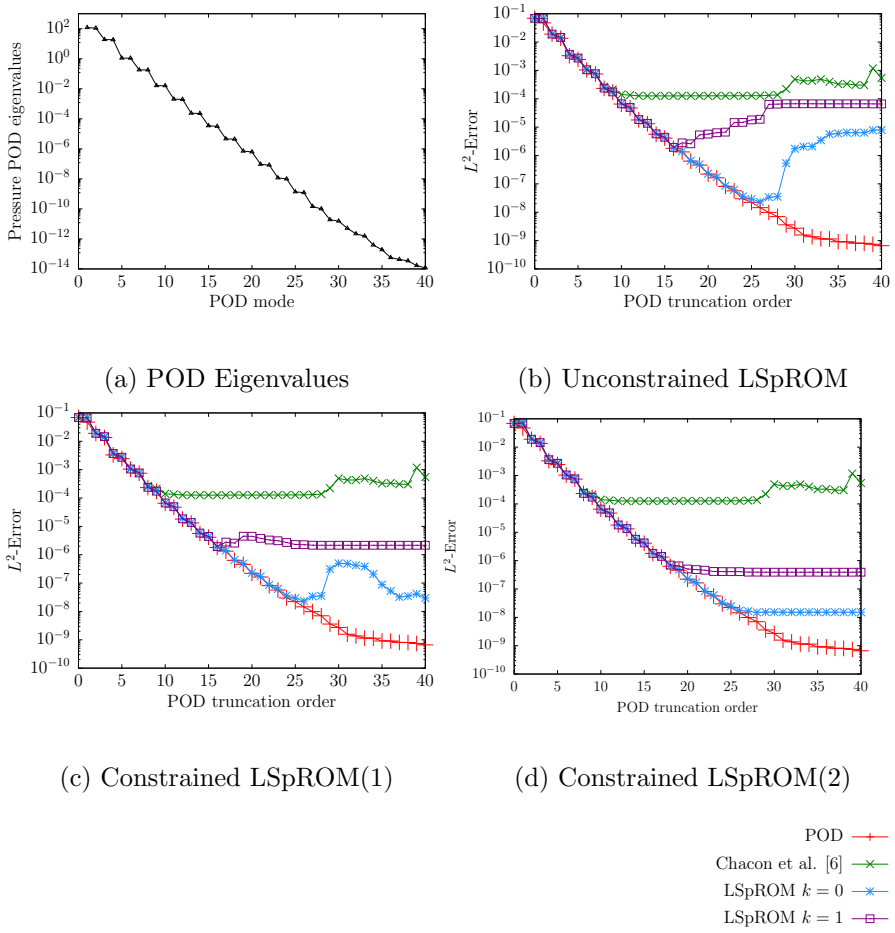

(a) POD Eigenvalues

(b) Unconstrained LSpROM

(c) Constrained LSpROM(1)

(d) Constrained LSpROM(2)

Figure 2: Pressure errors for the flow past a cylinder at $Re = 100$.

We also see a clear advantage for the LSpROM with the choice of $k = 0$, that provides reductions of errors of two to three orders of magnitude compared to $k = 1$. One way to explain this can come from the error estimates (41) (corresponding to $k = 0$) and (42) (corresponding to $k = 1$). In the latter the time derivative of the velocity error appears, which is not bounded by the L^2 POD that we are using. Finally, we note that for $k = 0$, the results are close to the projection error by the POD (curves in red), which is the optimal error that can be obtained.

To conclude this test case, we propose supplementing this quantitative study with a qualitative evaluation. We consider pressures enriched by 40 POD modes and calculated using the different

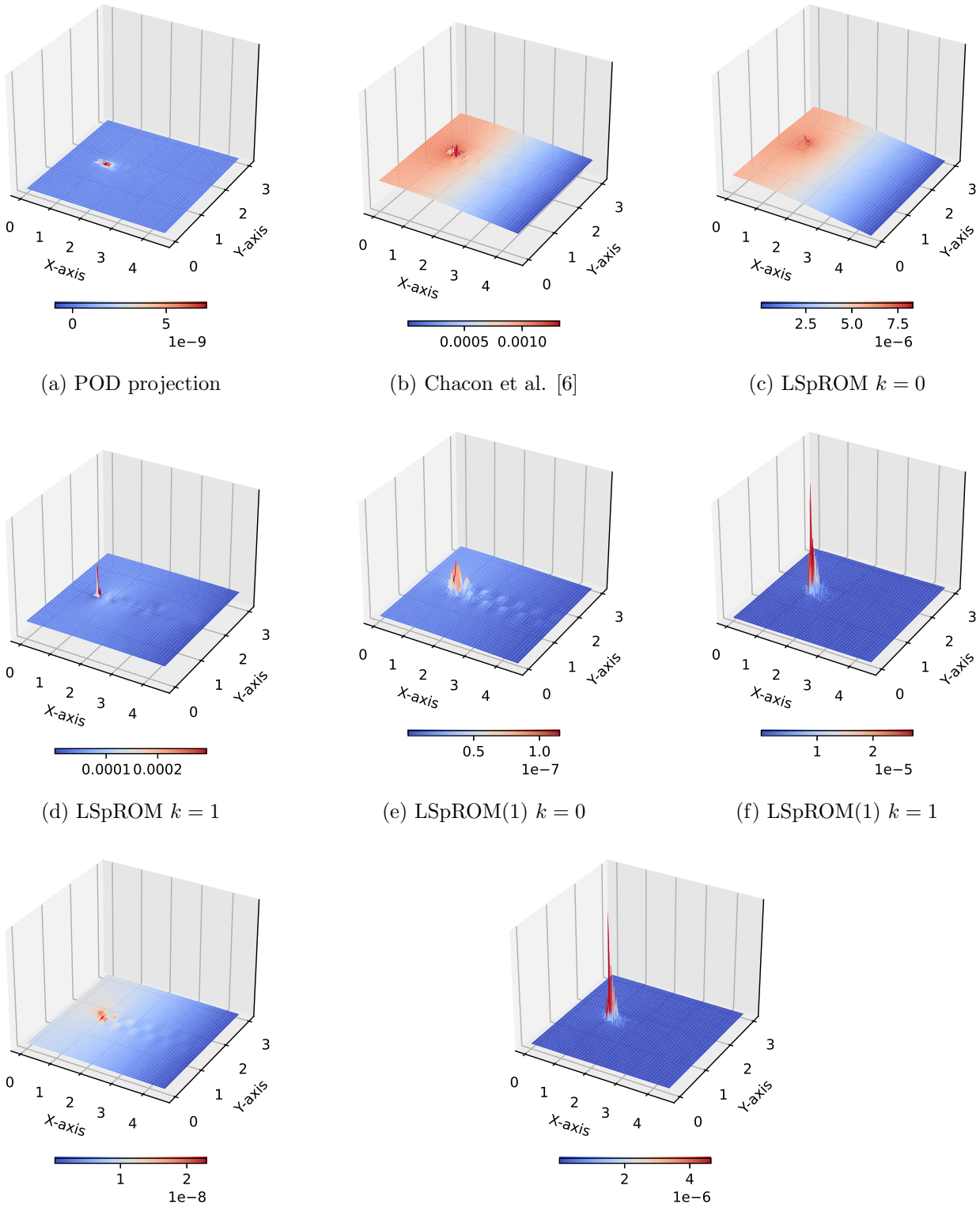

(a) POD projection (b) Chacon et al. [6] (c) LSpROM $k = 0$

(d) LSpROM $k = 1$ (e) LSpROM(1) $k = 0$ (f) LSpROM(1) $k = 1$

(g) LSpROM(2) $k = 0$ (h) LSpROM(2) $k = 1$

Figure 3: Pressure mean absolute error of the cylinder flow $Re = 100$

versions. Figures 3 show the pressure mean absolute error and its isovalues. The solution using LSpROM(2) with k=0 has an error level comparable to the POD projection. The error field illustrates the effectiveness of choosing LSpROM(2) with k=0 compared to the others.

Flow in a lid driven cavity Re = 10000.

The flow is considered in a cavity of square shape $]0, D[\times]0, D[$ where the fluid is driven by a tangential velocity of magnitude U applied to its top wall. No-slip conditions are imposed on the remaining walls. To perform the numerical computations, we used a triangular mesh composed of 32928 cells and a first order semi-implicit Euler scheme of step $\Delta t = 10^{-3}$ for time integration. The resulting flow is cyclic, where in the lower and upper left corners, the secondary vortex separates into two small vortices that periodically reincorporate. These structures are illustrated in Figure 4

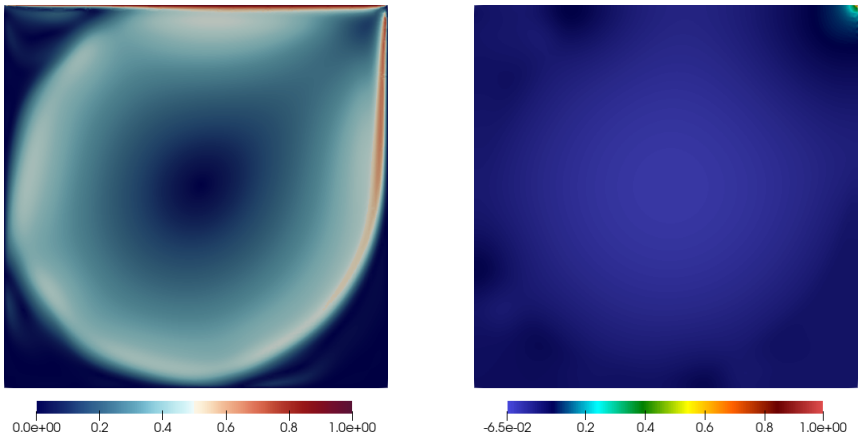

(a) Velocity (b) Pressure

Figure 4: High fidelity velocity and pressure solutions of the cavity flow, $Re = 10000$

Here again in order to construct the velocity and pressure POD bases, 200 uniformly distributed snapshots covering 8 periods of the periodic regime of the flow are considered.

Results and discussion From the top left subfigures of Figures 5, we can already see that the eigenvalues of the POD corresponding to the pressure decrease exponentially to zero. We come to the same conclusions as for the previous test cases. The figure 5 illustrates these results. In particular, the obvious improvement takes place for the constrained LSpROM 2, that provides a nearly monotonic decrease of errors as the number of POD modes increases (see the bottom right subfigures of Figures 5). We also see a clear advantage for the LSpROM with the choice of $k = 0$, that provides reductions of errors of two to three orders of magnitude compared to $k = 1$. Once more we note that for $k = 0$, the results are close to the projection error by the POD (curves in red), which is the optimal error that can be obtained.

As for the first case first, we propose to complete this quantitative study with a qualitative evaluation. We consider the pressures enriched by 40 POD modes and calculated with the different versions presented above. In Figures 6 we present respectively, the pressure mean absolute error and its isovalues. We observe that the solution obtained using LSpROM(2) and k=0 offers an error level of the same order as that of the POD projection.

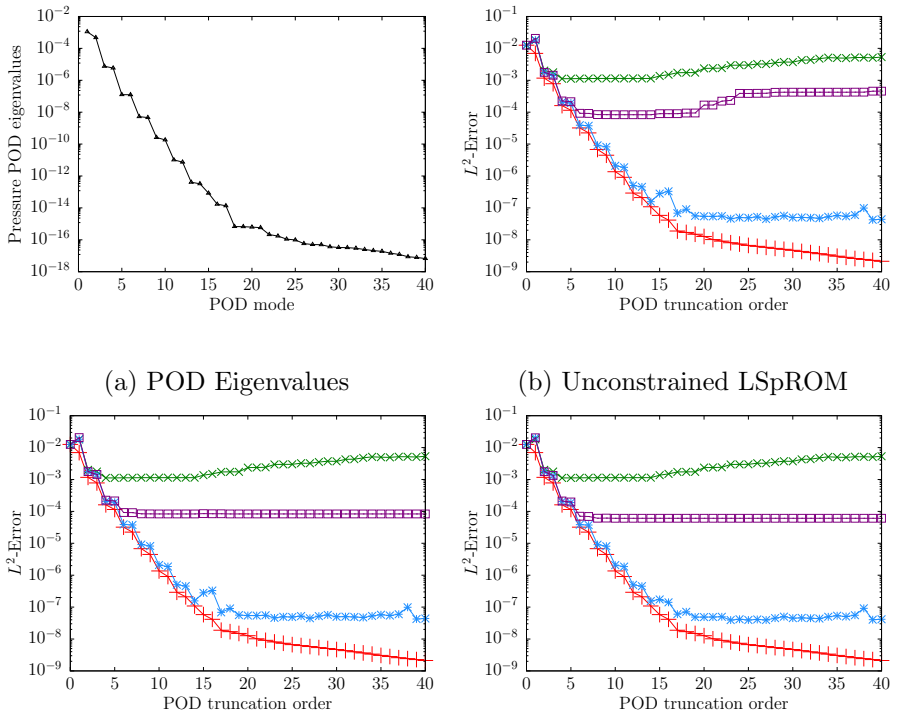

(a) POD Eigenvalues

(b) Unconstrained LSpROM

(c) Constrained LSpROM approach 1

(d) Constrained LSpROM approach 2

Figure 5: Pressure errors for the flow in a Lid Driven Cavity $Re = 10000$.

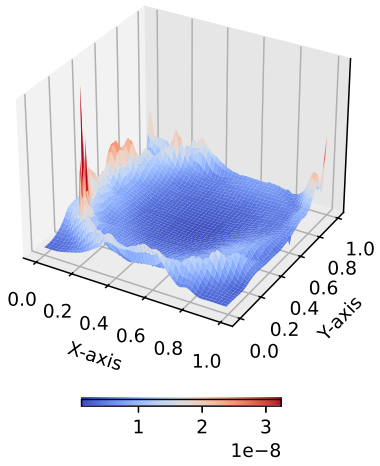

(a) POD

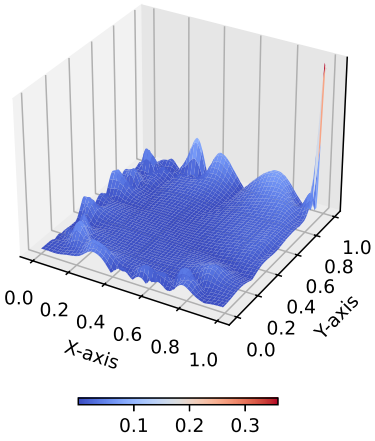

(b) Chacon et al. [6]

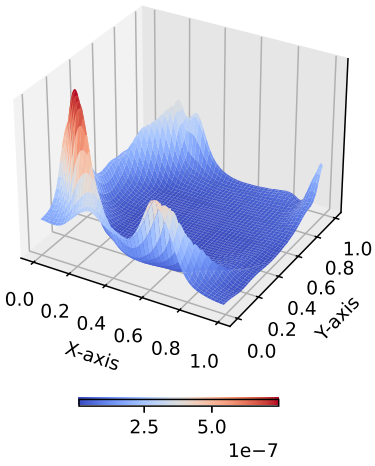

(c) LSpROM $k = 0$

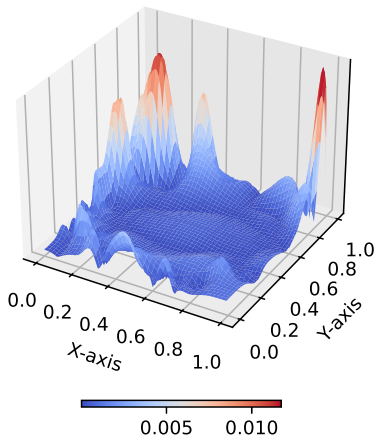

(d) LSpROM $k = 1$

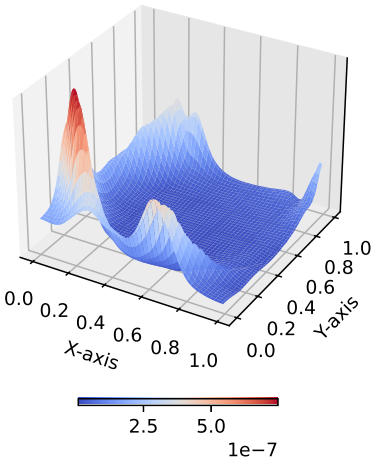

(e) LSpROM(1) $k = 0$

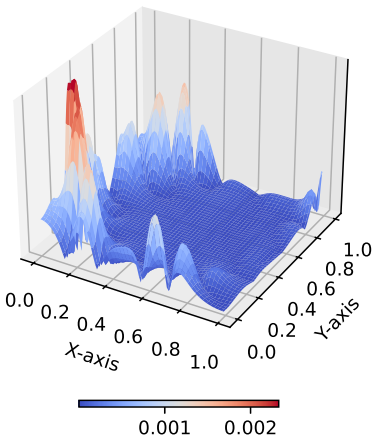

(f) LSpROM(1) $k = 1$

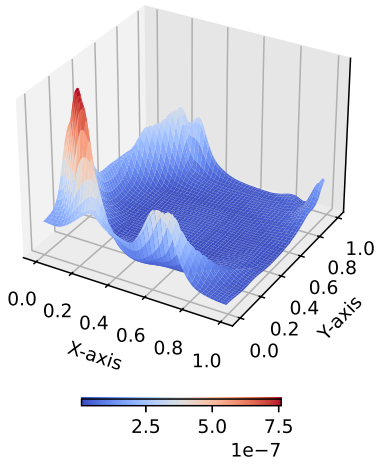

(g) LSpROM(2) $k = 0$

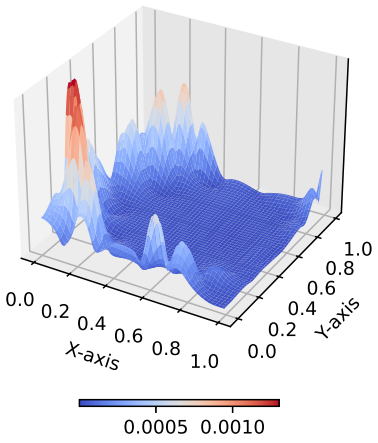

(h) LSpROM(2) $k = 1$

Figure 6: Pressure mean absolute error of the cavity flow $Re = 10000$

Singular pressure test case

In this final example, we push to the limite the pressure recovery by proposing to test the robustness of the LSpROM approaches on a specific complex fabricated case. We aim to recover the reduced pressure solution that is both highly singular and requires an impractically fine mesh for its approximation. We therefore propose to consider the velocity solution

$$\mathbf{u} = \sum_{k=1}^{20} 10^{-5}\, 2^{(20-k)}\, \cos(kt) \begin{bmatrix} \sin^2(k\,\pi\,x)\, \sin(2\,k\,\pi\,y) \\ -\sin(2\,k\,\pi\,x)\, \sin^2(k\,\pi\,y) \end{bmatrix} \tag{50}$$

while the pressure is an approximation of the Weirstrass function, which is continuous and nowhere differentiable

$$p = \sum_{k=1}^{20} 10^{-2} \left(\frac{4}{3}\right)^{(20-k)} \sin(k\,t)\cos(k\,t^{3/2}) \sum_{n=1}^{35} \left(\frac{1}{2}\right)^{n} (\cos((k+2)^n x) + \cos((k+2)^n y)) \tag{51}$$

To illustrate the irregularity of the pressure solution, three snapshots with a horizontal cut at $y = \frac{1}{2}$ corresponding to $t = 4$, $t = 8$ and $t = 12$ are plotted in figure 7.

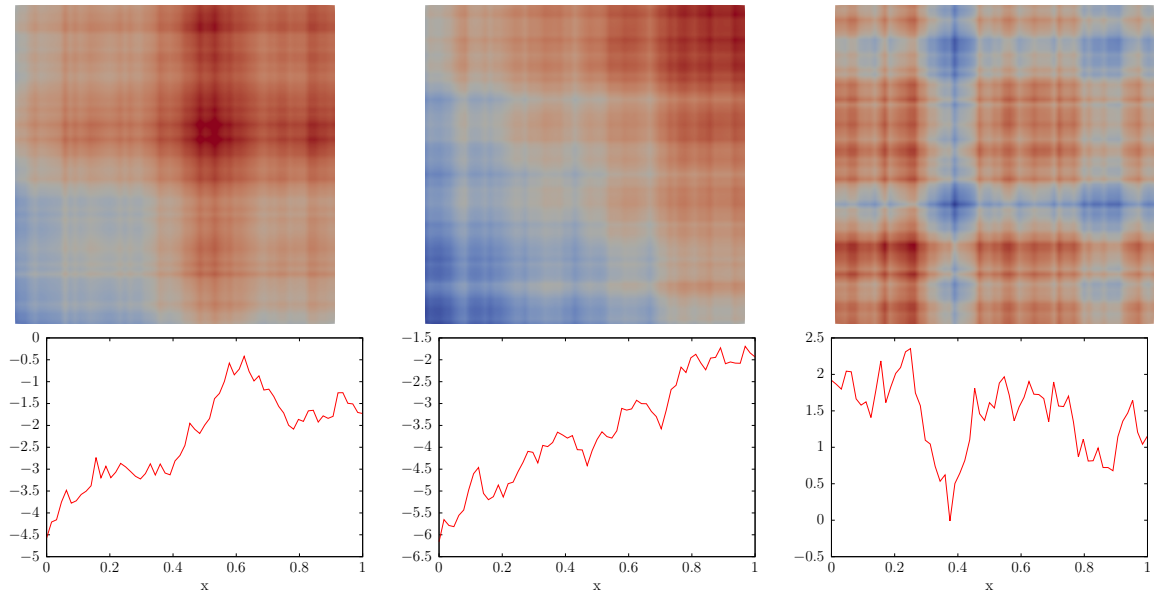

Figure 7: Illustration of the analytical truncated Weirstrass pressure scalar fields with a horizontal cut at $y = \frac{1}{2}$, in three times instances $t = 4$, $t = 8$ and $t = 12$.

Since pressure acts as a Lagrange multiplier to ensure the divergence free constraint, the challenge of developing pressure recovery schemes is equally important in the context of unsteady linear Stokes equations. We therefore propose to present our results both for the unsteady Stokes and for the Navier-Stokes equations. Moreover it will also allow us to appreciate the effect of nonlinear terms on the level of approximation of the reduced pressure.

Before we start the discussion on the numerical results, it is important to note that the irregularity of the selected pressure excludes the Laplacian-type method of Chacon et al. [6] that suggest the

pressure to be in H^1. Therefore, the next results will only be achievable using the proposed LSpROM technique capable of recovering the reduced pressure in L^2. Finally, regard to the previous numerical experiments, we chose to focus and show only the results using LSpROM(2).

Results and discussions : Using the given analytical solutions, the source term is calculated and the problem is solved in a domain $\Omega =]0,1[\times]0,1[$, with a regular triangular mesh of size 64×64 and for in time window $[0, 12]$. A choice of the viscosity is made to $\nu = 10^{-2}$ and a first order semi-implicit Euler scheme with step $\Delta t = 10^{-3}$ is used for time integration. The POD bases are afterwards built with snasphots uniformally retrieved from the simulations with a time jump of $100\Delta t$.

Unlike in the two previous cases, the convergence of the pressure POD eigenvalues towards zero is less evident. Figure 8 shows that for both unsteady Stokes and Navier Stokes snapshots, there is slow decay of pressure POD eigenvalues towards zero with a stagnation at a level around 10^{-6} achieved after a significant number of truncation modes. This indicates that a large number of modes is necessary to accurately capture the irregular structures present in the given Weirstrass pressure.

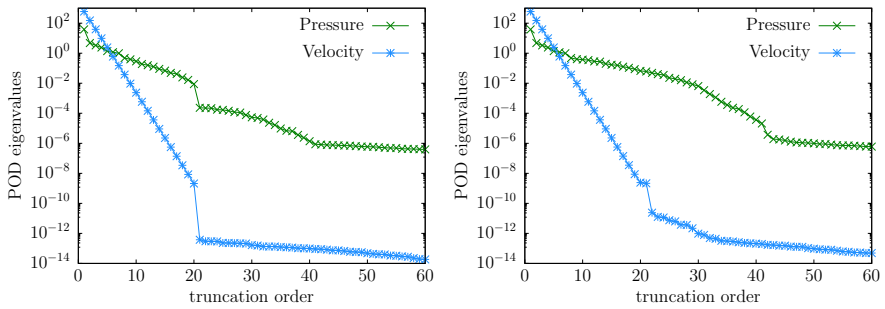

(a) Stokes case (b) Navier Stokes case

Figure 8: POD eigenvalues for the unsteady Stokes (left) and unsteady Navier-Stokes (right)

Pressure approximation errors presented in Figure 9 exhibit a conforming decay with respect to the POD number of modes up to the truncation order 20.

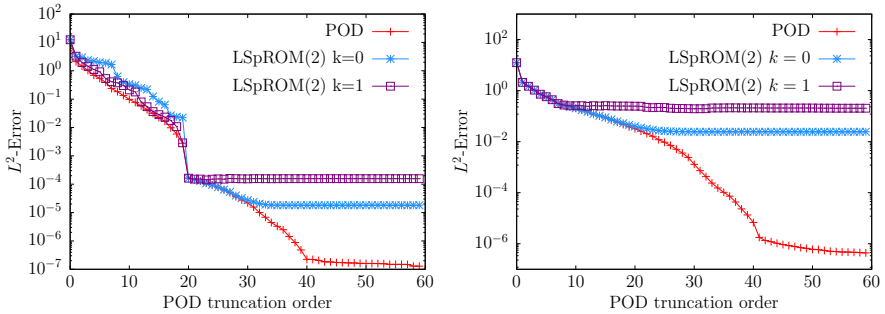

(a) Stokes case (b) Navier Stokes case

Figure 9: Pressure errors using constrained LSpROM approach 2: unsteady Stokes (left) and unsteady Navier-Stokes (right) .

This behavior is observed consistently across LSpROM approaches for $k = 0$ and for $k = 1$. For higher mode numbers, a stagnation in error reduction is noted for both unsteady Stokes and Navier Stokes cases. We can also note that the level of error approximation for the Navier Stokes is a thousand times larger than that obtained for Stokes. However for both problems, the obtained errors predictions align with the result predicted by theorem 5.1. Furthermore, one can note a difference in the error magnitude between the LSpROM(2) for $k = 0$ and $k = 1$. Ended, choosing $k = 0$ outperforms $k = 1$ by nearly an order of magnitude. This order gap underscores once again the superior performance of the choice $k = 0$ approach in maintaining lower error levels.

7 Conclusions

In this paper we have introduced a method to recover the reduced pressure for incompressible flows. We have given some fundamental theoretical results concerning the existence and uniqueness of the solution whenever the full-order pair of velocity-pressure spaces is inf-sup stable, and we have proved an optimal error estimate for the reduced pressure.

An additional highlight lies in the fact that our method is equivalent to solving the reduced mixed problem with reduced velocity basis enriched with the supremizers of the reduced pressure gradients.

We have introduced a constrained treatment to avoid instabilities for high number of modes, that provide nearly-optimal errors, close to the POD projection ones, that provide error reductions of four order of magnitudes with respect to the pressure Poisson equation procedure. All our theoretical results have been confirmed by numerical experiments on stiff test cases. We have specifically demonstrated, using a manufactured solution, the difference in pressure calculation levels for the Stokes and Navier-Stokes problems. This highlights the impact of the non-linear terms on the recovery procedure.

Acknowledgements

The research of M. Azaiez has been supported by the French National Research Agency ANR-23-ASTR-0003 (SINRAM). The research of T. Chacón and I. Sánchez has been partially supported by the Spanish Research Agency and EU Feder Fund Grant RTI2018-093521-B-C31, as well as the Marie Sklodowska-Curie Action 872442 MSCA-RISE-2019 "ARIA" Project.

References

[1] A. Abdulle and O. Budać, A Petrov-Galerkin reduced basis approximation of the Stokes equation in parameterized geometries, C. R. Math., 353 (2015), pp. 641-645, https://doi. org/10.1016/j.crma.2015.03.019.

[2] I. Akhtar, A. Nayfeh, C. Ribbens. *On the stability and extension of reduced-order Galerkin models in incompressible flows.* Theoret. Comput. Fluid Dyna. 23, 213-237 (2009). https://doi.org/10.1007/s00162-009-0112-y.

[3] F. Ballarin, A. Manzoni, A. Quarteroni, G. Rozza. *Supremizer stabilization of POD-Galerkin approximation of parametrized steady incompressible Navier-Stokes equations.* Int. J. Numer. Methods Eng. 102(5), 1136-1161 (2015).

[4] A. Caiazzo, T. Iliescu, V. John, S. Schyschlowa. *A numerical investigation of velocity-pressure reduced order models for incompressible flows.* J. Comput. Phys. 259, 598-616 (2014).

[5] K. Carlberg, C. Farhat, J. Cortial, D. Amsallem. *The GNAT method for nonlinear model reduction: effective implementation and application to computational fluid dynamics and turbulent flows.* J. Comput. Phys. 242, 623-647 (2013).

[6] T. Chacón Rebollo, S. Rubino, M. Oulghelou, C. Alléry. *Error analysis of a residual-based stabilization-motivated POD-ROM for incompressible flows.* Comput. Methods Appl. Mech. Engrg. 401, 115627 (2022).

[7] Y. Choi and K. Carlberg, Space-time least-squares Petrov-Galerkin projection for nonlinear model reduction, SIAM J. Sci. Comput., 41 (2019), pp. A26-A58, https://doi.org/10.1137/ 17M1120531.

[8] E. Fonn, H. van Brummelenb, T. Kvamsdalac, A. Rasheeda. *Fast divergence-conforming reduced basis methods for steady Navier-Stokes flow.* Comput. Methods Appl. Mech. Engrg. 346, 486-512 (2019).

[9] V. Girault, P.A. Raviart. *Finite Element Approximations of the Navier-Stokes Equations.* Springer, New York, 1986.

[10] P. M. Gresho, R. L. Sani. *On pressure boundary conditions for the incompressible Navier-Stokes equations.* Internat. J. Numer. Methods Fluids. 7, 1111-1145 (1987). https://doi.org/ 10.1002/fld.1650071008.

[11] J. L. Guermond, P. Minev, J. Shen. *An Overview of projection methods for incompressible flows.* Comput. Methods Appl. Mech. Engrg. 195, 6011-6045 (2006).

[12] Saddam Hijazi and Giovanni Stabile and Andrea Mola and Gianluigi Rozza. Data-Driven POD-Galerkin Reduced Order Model for Turbulent Flows. Journal of Computational Physics, V 416, page = 109513, 2020,

[13] G. Rozza, D. Huynh, A. Manzoni, Reduced basis approximation and a posteriori error estimation for Stokes flows in parametrized geometries: roles of the inf-sup stability constants, Numerische Mathematik 125 (1) (2013) 115-152.

[14] T. Iliescu, Z. Wang. *Are the snapshot difference quotients needed in the Proper Orthogonal Decomposition?* SIAM Journal on Scientific Computing, 36(3), A1221-A1250 (2014).

[15] A. Ivagnes, G. Stabile, A. Mola. *Pressure data-driven Variational Multiscale Reduced Order Models.* Journal of Computational Physics. 476, 111904 (2023). https://doi.org/10.1016/j.jcp.2022.111904.

[16] , K. Kean, M. Schneier. *Error analysis of supremizer pressure recovery for POD based Reduced- Order Models of the time-dependent Navier-Stokes equations.* SIAM Journal on Numerical Analysis. 58(4), 2235-2264 (2020).

[17] B. Koc, T. Chacón Rebollo, S. Rubino. *Uniform bounds with difference quotients for Proper Orthogonal Decomposition Reduced Order Models of the Burgers Equation.* Journal of Scientific Computing. 95, 43 (2023). https://doi.org/10.1007/s10915-023-02160-2.

[18] H. P. Langtangen, A. Logg. *Solving PDEs in Python: The FEniCS Tutorial I.* Springer Publishing Company, Incorporated, 1st edition (2017).

[19] M. Mohebujjaman, L. G. Rebholz, T. Iliescu, Physically-constrained data-driven correction for reduced order modeling of fluid flows, Int. J. Num. Meth. Fluids 89 (3) (2019) 103-122.

[20] B.R. Noack, P. Papas, P. A. Monkewitz. *The need for a pressure-term representation in empirical Galerkin models of incompressible shear flows.* J. Fluid Mech. 523, 339-365 (2005).

[21] N. C. Nguyen, K. Veroy, A.T. Patera. *Certified real-time solution of parametrized partial differential equations.* R. Catlow, H. Shercliff and S. Yip editors, Handbook of materials modeling, Kluwer Academic, 2005.

[22] A. Quarteroni, G. Rozza. *Numerical solution of parametrized Navier-Stokes equations by reduced basis methods.* Numer. Methods Partial Differential Equations, 23, 923-948 (2007).

[23] A. Quarteroni, F. Saleri, A. Veneziani. *Factorization methods for the numerical approximation of Navier-Stokes equations.* Comput. Methods Appl. Mech. Engrg. 188(1), 505-526 (2000).

[24] A. Quarteroni, A. Valli. *Numerical approximation of partial differential equations.* Springer, Berlin, 1994.

[25] D. V. Rovas. *Reduced-Basis output bound methods for parametrized partial differential equations.* Ph D Thesis, Massachussets Institute of Technology, 2003.

[26] G. Rozza, K. Veroy. *On the stability of the reduced basis method for Stokes equations in parametrized domains*. Comput. Methods Appl. Mech. Engrg. 196(7), 1244-1260 (2007).

[27] R. L. Sani, J. Shen, O. Pironneau, P. M. Gresho. *Pressure boundary condition for the time-dependent incompressible Navier?Stokes equations*. J. Numer. Methods Fluids. 50, 673-682 (2006). https://doi.org/10.1002/fld.1062.

[28] G. Stabile, S. Hijazi, A. Mola, S. Lorenzi, G. Rozza. *POD-Galerkin reduced order methods for CFD using finite volume discretisation: vortex shedding around a circular cylinder*. Commun. Appl. Ind. Math., 8 (2017), https://content.sciendo.com/view/journals/caim/8/1/article- p210.xml.

[29] R. Temam. *Navier Stokes equations*. North Holland, Amsterdam, 1984.

[30] F. Eivind, H. Brummelen, T. Kvamsdal, and A. Rasheed, Fast divergence-conforming reduced basis methods for steady Navier-Stokes flow, Comput. Methods Appl. Mech. and Engrg., 346 (2019), pp. 486-512, https://doi.org/10.1016/j.cma.2018.11.038.